2013-03-22

Immobilized Viologen Polymer for Use in Direct Carbohydrate Fuel Cells

Yining Pan
Brigham Young University - Provo

Immobilized Viologen Polymer for Use in Direct Carbohydrate Fuel Cells

Yining Pan

A thesis submitted to the faculty of
Brigham Young University
in partial fulfillment of the requirements for the degree of

Master of Science

Dean R. Wheeler, Chair
William G. Pitt
Thomas A. Knotts

Department of Chemical Engineering

Brigham Young University

February 2013

ABSTRACT

Immobilized Viologen Polymer for Use in
Direct Carbohydrate Fuel Cell

Yining Pan
Department of Chemical Engineering, BYU
Master of Science

Glucose and other carbohydrates are some of the most abundant renewable energy sources in the world. The oxidation of carbohydrates in a fuel cell allows their chemical energy to be converted directly into electrical energy. Viologen has been indentified and shows promising ability as an electron-transfer catalyst or mediator for carbohydrate oxidation in an alkaline carbohydrate fuel cell. Building on the previous results, the objective of this work was to develop an immobilization chemistry of viologen onto an electrode and to investigate the catalytic activity for carbohydrate oxidation in direct carbohydrate fuel cells.

The immobilization was achieved by electropolymerizing a novel viologen monomer onto an electrode surface. The novel viologen monomer, which functions as a monosubstituted viologen, was synthesized and isolated in-house. Gold-plated nickel wire and graphite disks were used as the substrates for the electropolymerization. SEM, EDAX, XPS and water-contact-angle measurement were used to verify the formation of the coating on the gold and graphite surfaces. The catalytic activity of the immobilized viologen on graphite disk surface was examined using a fuel-cell-like device. The test was operated within the desired pH range for an operating fuel cell; it was found that the immobilized viologen polymer has a low catalytic activity toward oxidizing carbohydrates.

In addition, the electrochemical properties of the novel viologen monomer were investigated by the method of cyclic voltammetry, as well as for that of two aminoviologens synthesized in-house. Redox potentials, diffusion coefficients, and heterogeneous electron-transfer rate constants were determined.

Keywords: viologen, electropolymerization, fuel cell, voltammetry

ACKNOWLEDGEMENTS

I would like to show my gratitude to my advisor and mentor Dr. Wheeler, who helped and guided me for the past two and half years. To my second advisor Dr. Pitt, who provided the good advice and support to this work.

I am obliged to many of my colleagues who helped me, including Dr. Dane Hansen, James Stockton, Russ Urie, and Chien-Wei Chao.

I would like to thank my dear husband Lingfu (Larry) Zhang, the love of my life, for his personal support and great patience at all times.

And finally, to the Lord, who encouraged and gave me help along the way, and blessed me with the strength to finish this journey.

Table of Contents

List of Tables

List of Figures

1 Introduction

1.1 Motivation

Glucose and other carbohydrates have been recognized as alternative fuel sources to supplement fossil fuels as carbohydrates are plentiful, renewable, and convenient, while having high energy density [1-3]. We envision the use of carbohydrates as energy sources in biomass-rich and regions of the world that have a poorly developed energy grid, and for powering bio-implantable medical devices. This work aims to convert chemical energy stored in carbohydrates into electrical energy.

Fuel source Glucose molecular units are present in all kinds of plants and crops, and are one of the most abundant bimolecular units on the earth. Starchy materials, such as corn, potato, cassava and many others, contain glucose units and are the most used feedstock for glucose production [4]. Commercially, glucose is directly produced from hydrolysis of starch. Because starchy materials are in the human food chain, they can be expensive and compete with the global food supply. Alternatively, glucose can be made from cellulosic materials, such as paper, wood, and other fibrous plant materials, like grass [5]. Cellulosic resources are in general very widespread and abundant, and unlike starchy materials, they are not competitive with the global food supply. And yet, this technology is not commercially practical because of the high cost for extracting the glucose from the encapsulated cellulose molecules [5].

The most common route to utilize carbohydrates, e.g. glucose, as an energy source is fermentation to ethanol for use in internal combustion engines. In the United States, over 90% of fuel ethanol is produced from starchy materials [6]. The glucose as the intermediate product made through ethanol production can be also used in carbohydrate fuel cells. The advantage of glucose over ethanol as a fuel is elimination of the fermentation step. By the end of 2012, the ethanol wholesale price was $0.86 per kg [7]. In comparison, the wholesale price for raw sugar is $0.56 per kg [8]. This is for sucrose, but should be roughly equivalent to glucose. During the fermentation of glucose to ethanol, 1 mole of glucose is used to produce 2 moles of ethanol, and the efficiency is 85% [5]. When the glucose oxidation goes to completion, the available energy is 16 MJ/kg of glucose [9]. For the equivalent of ethanol produced from 1 kg glucose, the available energy is 12.9 MJ when the oxidation of ethanol goes to completion. Thus, glucose provides greater energy value than does ethanol produced from glucose.

Using carbohydrates as an energy source or fuel could have value in certain situations, such as areas where biomass is rich and the electric grid is lacking. The subject of this work is converting carbohydrates into electrical energy. At this point the process does not have high efficiency and would not be commercially viable. However, it is still at the early stage of this technology, and it is not clear how efficient it may eventually become.

Glucose fuel cells The oxidation of carbohydrates in a fuel cell allows their chemical energy to be converted directly into electrical energy. It is a more energy-efficient process to extract energy from biomass in the form of electricity. There are some lengthy reviews describing glucose as a potential fuel for fuel cells [10-12]. The first article on glucose as fuel for fuel cells was published in 1964, using an enzyme as catalyst [13]. Since then, other researchers

have been focused on using precious metals, transition metals, or bacteria as catalysts to facilitate the glucose oxidation.

Enzymatic glucose oxidation has being studied for powering implanted medical devices [10, 13]. But it is an inefficient process and can only extract 2 electrons out the available 24 electrons from one single glucose molecule. Metal catalysts, such as platinum, release electrons from glucose [14-16], but platinum is very costly and at this time cannot be economically used in a large-scale plant, and has a low conversion rate. Bacteria can liberate nearly all the 24 electrons from glucose oxidation in a carbohydrate fuel cell; however, this technology achieves a low power output and is therefore not commercially viable for large-scale electrical energy production [17-19] .

Viologen as catalyst Organic compounds called viologens, derivatives of 4,4'-bipyridyl, have been identified and show promising ability as electron-transfer catalysts or mediators to oxidize carbohydrates under alkaline conditions. When viologens are reduced they exhibit an intense blue color, and this is where the compounds got their name. This class of compounds can undergo a reversible redox process without permanent alteration. Homogenous viologen catalysts are the basis for the anode in a cell that generated quasi-steady-state current up to 30 mA/cm^2 using fructose as fuel and produced a power output of 15 mW/cm^2 [20].

The tested viologens are able to oxidize carbohydrates in a homogenous solution. However, viologens has an oral toxicity to humans, it is undesirable to release viologens into the environment with the fuel cell waste. Such release would also increase the fuel cost. Therefore, the viologens must be immobilized onto an electrode surface to make an inexpensive and environmentally friendly fuel cell device. Moreover, the immobilization can increase efficiency

of the fuel cell, as the viologens have intimate contact with the anode current collector, and thus are prevented from crossing over to the cathode side.

1.2 Scope

The primary goal of this work is to develop immobilization chemistry of viologen molecules on electrode surfaces as electron-transfer catalysts for use in direct carbohydrate fuel cells and to quantify the electrochemical activity of the catalyst. These steps will allow an improvement in the fuel cell efficiency.

Chapter 2 provides background and basic understanding of this research, including an introduction to low-temperature fuel cells, direct carbohydrate fuel cells (DCFC), and basic electrochemical experimental techniques. Viologens are introduced in Chapter 2. Also included are some prior results at BYU investigating soluble viologens for use in a DCFC, as well as a review and discussion of existing viologen polymers.

There are two key questions to be answered in this work: (1) how to immobilize viologen molecules on an electrode surface, e.g. graphite surface or gold surface, and (2) how electroactive is the viologen-modified electrode surface toward oxidizing carbohydrates under alkaline conditions.

In order to immobilize viologens on an electrode surface, a novel viologen molecule is made and polymerized by a means of electropolymerization. The structure of the novel viologen molecule was chosen guided by the prior results discussed in Chapter 2. The synthesis of this novel viologen monomer is presented in Chapter 3. Detailed experimental reaction steps are included, as well as the separation of the pure material from the raw product. The novel viologen monomer is identified using NMR and mass spectrometry. Chapter 3 also includes synthesis and

identification of another two new types of viologen molecules, namely aminopropyl viologen (APV) and methylaminopropyl viologen (MAV), which were used to study the suitability of monosubstituted viologen for use in DCFCs in Ref [21].

Chapter 4 includes the electrochemical investigation of APV, MAV and the novel viologen monomer using a standard electrochemical method known as cyclic voltammetry. Chapter 5 discusses the immobilization of the viologen monomer by electropolymerization on gold and graphite surfaces. The polymerization was verified by scanning electron microscopy (SEM), EDAX, and water contact angel. Subsequently, experiments were completed to answer the second key question, that is if the viologen modified electrode surface is electroactive and to what degree can oxidize carbohydrate molecules. A rotating disk electrode was used to test the degree of oxidizing carbohydrates. In addition, the electroactivity of the solubilized viologen monomer was also studied in a fuel-cell-like device. Conclusions and recommendations for future work are presented in Chapter 6.

2 Background

2.1 Introduction

To understand the research presented in this thesis it is helpful to first introduce some basics of direct carbohydrate fuel cells (DCFC), electrochemical experimental techniques, test apparatuses, and prior results at BYU upon which this research is based. Also included here is a brief summary of viologen-based polymers with a discussion of their potential advantages and disadvantages for use in a direct carbohydrate fuel cell.

2.2 Fuel Cells

Fuel cells are being developed for electric power generation and for transportation applications. They are devices that directly convert the chemical energy from a fuel into electricity through a chemical reaction with oxygen or another oxidizing agent. As long as a constant source of fuel and oxidizer are supplied, fuel cells can produce electricity continually.

There are many types of fuel cells, but the major ones include the solid oxide fuel cell (SOFC), phosphoric acid fuel cell (PAFC), molten carbonate fuel cell (MCFC), proton exchange membrane fuel cell (PEMFC), alkaline fuel cell (AFC), and direct methanol fuel cell (DMFC) [22]. Most of these types are commercially available today, though none are widely adopted. Each type has its own chemistry, operating temperature, catalyst, and electrolyte. Their operating characteristics help identify their applications; for example, low-temperature DMFCs and

PEMFCs are used for powering passenger vehicles, while larger high-temperature SOFCs, MCFCs and PAFCs are used for stationary power generation [23].

Fuel cells come in many various forms, but they all work in the same general manner. Figure 2.1 shows an operating PEM (hydrogen) fuel cell, which is a good example to illustrate most common features of different types of fuel cells. As seen in Figure 2.1, a fuel cell device is constructed with an anode and a cathode, spatially separated and in ionic contact with an electrolyte. The electrolyte serves to allow the current to be carried by ions while blocking the flow of electrons. Hydrogen, as fuel, enters the cell and is electro-oxidized at the anode, which liberates electrons. The liberated electrons flow through an external circuit, where they are used to power an external device, and then delivered to the cathode. In the mean time, the protons (H^+) produced from H_2 oxidation travel through the electrolyte to the cathode. At the cathode, the electrons meet with the protons and oxygen, which makes H_2O.

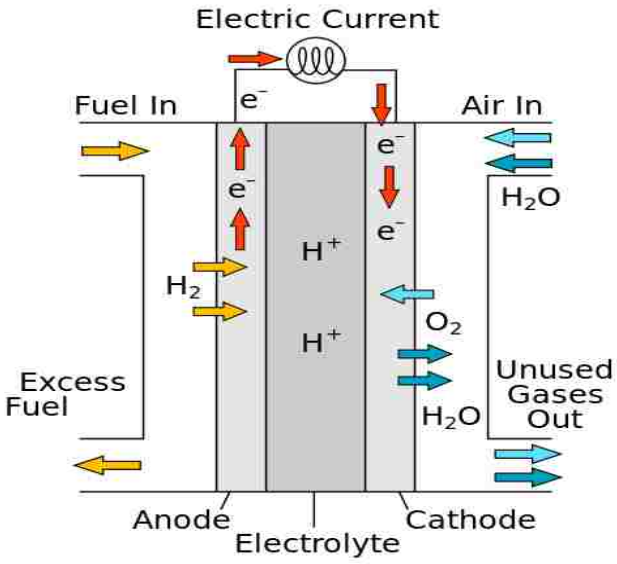

Figure 2.1 Scheme of a hydrogen operating fuel cell [23].

2.3 Direct Carbohydrate Fuel Cell

Direct carbohydrate fuel cells (DCFC) operate under the same concept as the hydrogen fuel cell above. Figure 2.2 is an idealized schematic of a generic alkaline DCFC with glucose as fuel. At the anode, glucose molecules react with OH^- to produce up to 24 electrons per glucose molecule. The electrons travel through an external circuit from the anode to the cathode where they are consumed by oxygen and water to form OH^-. The produced OH^- then travels through the electrolyte to the anode where it participates in the oxidation of glucose.

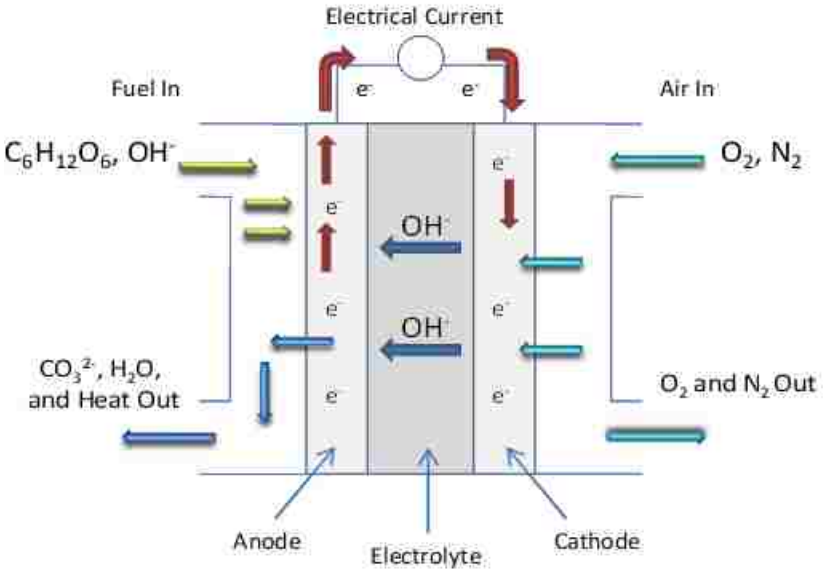

Figure 2.2 Schematic of an idealized alkaline direct carbohydrate fuel cell.

Equations 2.1 and 2.2 are a representation of the reactions occurring at the anode and cathode, respectively. Equation 2.3 is the overall equation where glucose is oxidized to carbonate and water.

Anode: $C_6H_{12}O_6 + 36\ OH^- = 6\ CO_3^{2-} + 24\ H_2O + 24\ e^-$ (2.1)

Cathode: $6\ O_2 + 12\ H_2O + 24\ e^- = 24\ OH^-$ (2.2)

Overall: $C_6H_{12}O_6 + 12\ OH^- + 6\ O_2 = 6\ CO_3^{2-} + 12\ H_2O$ (2.3)

The anode is where the oxidization of fuel occurs in an operating fuel cell. In the case of an alkaline DCFC, in order to generate useful current, a catalyst is required to speed up the oxidation of carbohydrates. Precious and transition metals are traditional catalysts operating under basic conditions, e.g. Pt. Our group found that viologens appeared to be more effective catalysts, because the traditional catalysts are very costly and the conversion rates are low [16, 24].

The cathode is where the oxygen reduction reaction (ORR) occurs. Non-precious-metal catalysts have been studied for the past 40 years to replace the traditional Pt-based catalyst for the ORR, in order to reduce the overall system cost [25]. Generally, these alternative catalysts require alkaline rather than acidic operating conditions. Carbon-supported non-precious-metals including transition metal oxides were showed to posses ORR activity under alkaline conditions [25-30]. For example, cobalt phthalocyanine (CoPc) was first demonstrated in 1964 for basic conditions and opened a new direction for research in the field of fuel cell catalysis [25]. A commercially available carbon-supported non-precious-metal catalyst is Electric Fuel's E-5 cobalt-based cathode; it was originally designed for use in Zinc-air batteries. This cathode material was used in our DCFC as discussed in Chapter 4.

2.4 Viologen

Viologen compounds are derivatives of 4,4'-bipyridyl and discovered over 75 years ago [31]. There are two types of viologens: disubstituted and monosubstituted. Methyl viologen is an example of the disubstituted type, which are N, N'-disubstituted- 4,4'-bipyridine salts [32].

Monomethyl viologen is an example of the monosubstituted type, which are N'-substituted- 4,4'-bipyridine salts. Both types can undergo a reversible redox process, where they are able to accept an electron and give it up without permanent alteration. In this case, disubstituted viologen can undergo two reversible redox steps, and monosubstituted can undergo one. Structures of representative viologens and redox processes discussed here are shown in Figure 2.3.

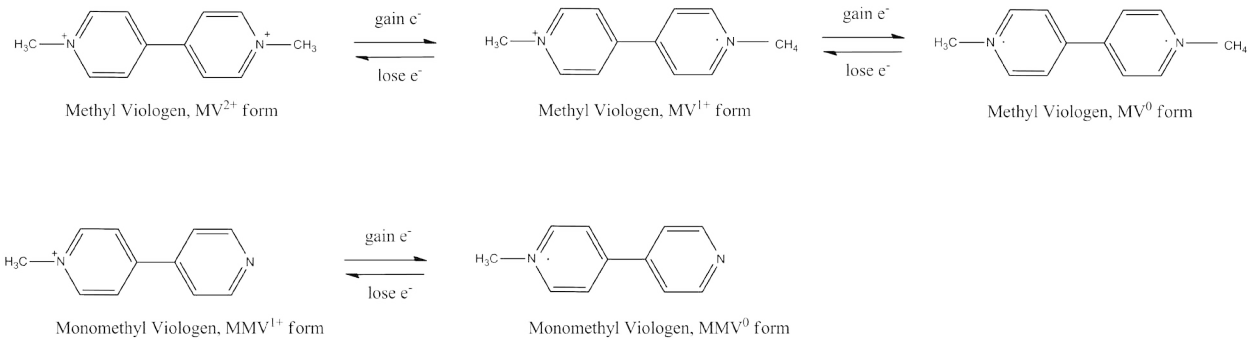

Figure 2.3 Structure of representative viologens discussed here and redox processes.

Disubstituted viologens have been studied extensively because of their interesting properties. The disubstituted viologens were originally investigated as a redox indicator in biological studies, possessing one of more cathodic redox potentials of organic systems showing a significant degree of reversibility [33]. Methyl viologen, also called "paraquat", was discovered for use as an herbicide. The herbicidal activity was found to be linked to the redox potential [34, 35]. Because of their electrochemically reversible behavior and the marked color change between the two oxidation states, viologens are favored candidates for electrochemical display devices as alternative to LEDs and LCDs [33]. On-going research also involves the investigation of disubstituted viologens for photoelectrochemical processes as their cation radicals have a strong optical absorption band in the visible region of the spectrum [36, 37].

However, monosubstituted viologens had received much less attention in the literature before our group started the investigation of viologen-catalyzed DCFC.

2.4.1 Anode Reactions in a Viologen-Catalyzed DCFC

With the presence of viologens, e.g. methyl viologens, as catalysts in an alkaline DCFC, the overall reaction (Equation 2.3) and the reaction occurring at the cathode (Equation 2.2) are unchanged. The reaction of glucose oxidation at the anode (Equation 2.1) is broken into two steps as given by Equation 2.4 and 2.5.

$$C_6H_{12}O_6 + 36\ OH^- + 24\ MV^{2+} = 6\ CO_3^{2-} + 24\ H_2O + 24\ MV^{1+} \quad (2.4)$$

$$24\ MV^{1+} = 24\ MV^{2+} + 24\ e^- \quad (2.5)$$

The oxidation of glucose is facilitated by MV^{2+} and causes MV^{1+} to be reduced. The reduced MV^{1+} is then oxidized back to its dicationic form by the anode current collector that is connected with the external circuit. Figure 2.4 shows MV shuttling electrons from glucose to anode.

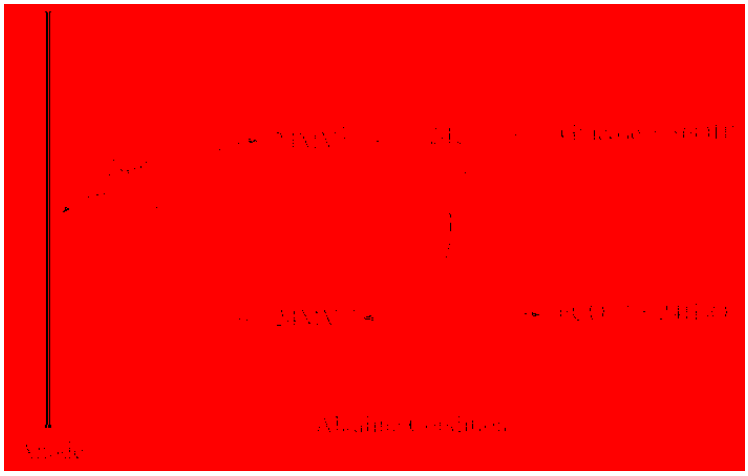

Figure 2.4 MV, as catalyst, facilitates glucose oxidation.

2.5 Prior Results of Viologen-Catalyzed DCFC

This work is an extension of previous research, carried out by a fellow PhD student, on the effectiveness and utility of viologen as a catalyst for use in DCFCs [1, 3, 9, 20, 21]. To understand the foundation of this work, it is necessary to introduce the prior results that this work is based on.

2.5.1 Pourbaix Diagram

In order to understand the electrochemical behavior of an alkaline DCFC system, it is helpful to construct and examine a Pourbaix diagram of the carbohydrates, as fuel, and viologens, as catalysts. The diagram for a generic carbohydrate fuel based on Ref [21] is shown in Figure 2.5. The potential difference between the reduced catalysts and the O_2 at the cathode is the open-circuit voltage (OCV) for the cell, and represents the electric potential available to the cell. Similarly, the difference in potential between the fuel and the catalyst is the driving force for the oxidation of the fuel by the catalyst. Both MV and MMV redox reactions are independent of pH values; however, there is a narrow range of pH values, namely 11-14, that are optimal to obtain a large potential output and, at the same time, to drive the oxidation of carbohydrates to completion.

MMV vs MV: Overall, MMV appears to be a more suitable catalyst than MV for our application. As illustrated in Figure 2.5, the redox potential of MMV is more negative than that of MV, showing -0.81V for MMV and -0.44 V for MV [21]. This leads to an open circuit potential of 1.33 V for MMV and 0.96 V for MV, indicating that MMV can retain a greater portion of the chemical energy of carbohydrates when converting into electrical energy. From the

previous study, at pH 12, about 90% of the energy in the carbohydrate fuel is retained if MMV is used as the catalyst, and about 66% of the energy is retained if MV is used [20].

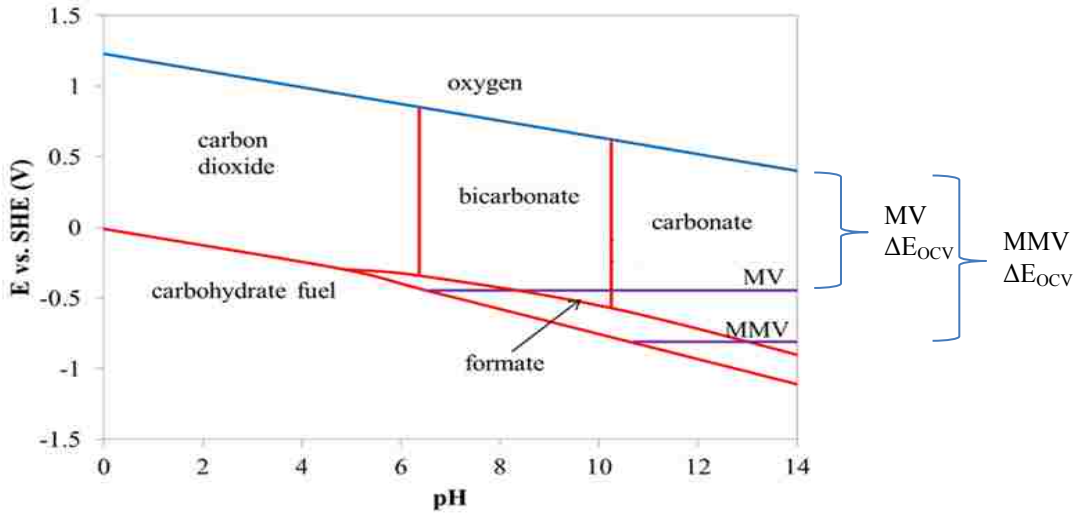

Figure 2.5 Pourbaix diagram for carbohydrate redox system, modified from Ref [21]. Included here are the redox potentials of methyl viologen (MV) and monomethyl viologen (MMV). The brackets show the values of open circuit voltage for MV and MMV, respectively.

In strong base, monosubstituted viologens were shown using mass spectrometry to be more stable than disubstituted viologens [20]. The stability of MMV in 1 M KOH was shown to be at least on the order of days. Whereas, within 20 minutes in 1 M KOH, the MV peaks in mass spectra begin to disappear, and within 48 hours the MV has no visible identification mass spectra peaks as they undergo hydrolysis and break into MMV.

However, the disubstituted viologens were found to react faster and more efficiently oxidize carbohydrates compared to monosubstituted viologens, by a factor of 1.2-1.5 under the same condition [20]. This may be due to the facts that the disubstituted viologens are stronger oxidants and have two quaternary positively charged centers. Comparing with the one quaternary positively charged center of monosubstituted viologens, the two quaternary positively charged

centers are more likely to facilitate interaction and subsequent oxidation of the negatively charged endiol form of the carbohydrates (See Figure 2.8) [3].

To summarize, the monosubstituted viologen exhibits somewhat slower kinetics, but has improved redox potential and stability compared to MV. The viologen monomer designed and synthesized in Chapter 3 is designed to mimic the advantages and structure of MMV.

2.5.2 Coulombic Efficiency

To study how the extent of carbohydrate oxidation depends on the catalyst-to-carbohydrate ratios, "sealed vial" tests were carried out in work prior to the present research [3]. In the "sealed vial" tests, methyl viologen and glucose were introduced into a pH-buffered solution in contact with air, and oxygen uptake was measured to determine the oxidation efficiency of glucose, and hence determine coulombic efficiency of the cell [1]. Figure 2.6 illustrates the results of this study. An efficiency of 100% corresponds a complete oxidation of glucose that produces 24 electrons. At the highest ratios (15 moles MV to 1 mole glucose) it appears that nearly all of the 24 electrons available in glucose are harvested.

To enhance the efficiency through increasing catalyst ratio, the use of viologen polymers appeared to be a promising approach. Soluble viologens in the form of polymers reported in Ref [3], as shown in Figure 2.7, were found to act 25% more efficiently on oxidizing carbohydrates than an equivalent concentration of native methyl viologen monomers. It was explained that polymeric viologens, whether immobilized or not, provide a high localized catalyst concentration and effect high viologen-to-carbohydrate ratios [3]. But the overall reaction rates for the free viologen polymers are slower, because they have poorer solubility in aqueous solution than the methyl viologens and interact with electrode more slowly. Due to the inherent transport

limitations, the polymers require heating to greater than 40 ºC during the process of oxidizing carbohydrates, and were found to be more susceptible to degradation at higher pH than methyl viologen monomers [3].

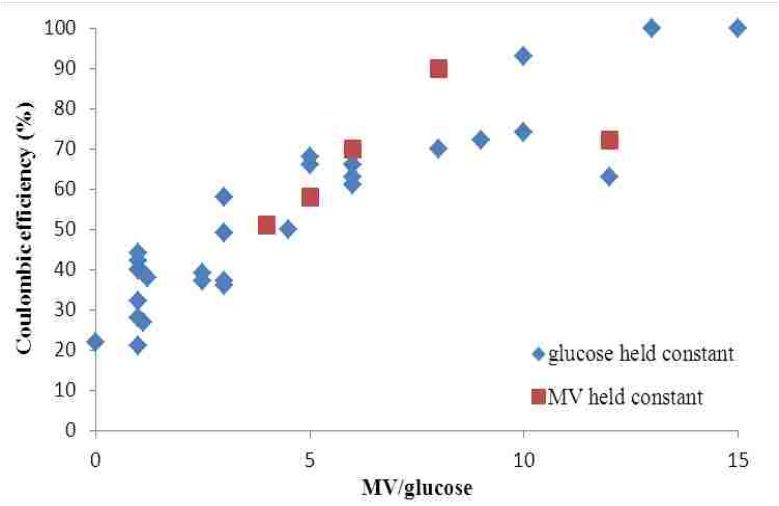

Figure 2.6 "Sealed vial" tests on efficiency of glucose oxidation by O2 with methyl viologen [1].

2.5.3 Carbohydrate Oxidation Mechanism

Prior result has proposed the alkaline oxidation mechanism of carbohydrate, e.g. glucose, which is demonstrated in Figure 2.8. There are two reaction pathways involved, as seen numbered in the figure. If there is enough viologen present that it can always accept the electrons, then the step-wise oxidation reaction will continue and follow Path 1 with the high coulombic efficiencies at the high catalyst ratios. Whereas, if not enough viologen is present, then the intermediates have time to rearrange into a terminal product, like tetrose carboxylate, and follow Path 2, resulting in lower coulombic efficiency. A high concentration of catalyst to fuel, at least 10 equivalent viologens to 1 carbohydrate, is required to minimize formation of unreactive intermediates in order to increase coulombic efficiency [3].

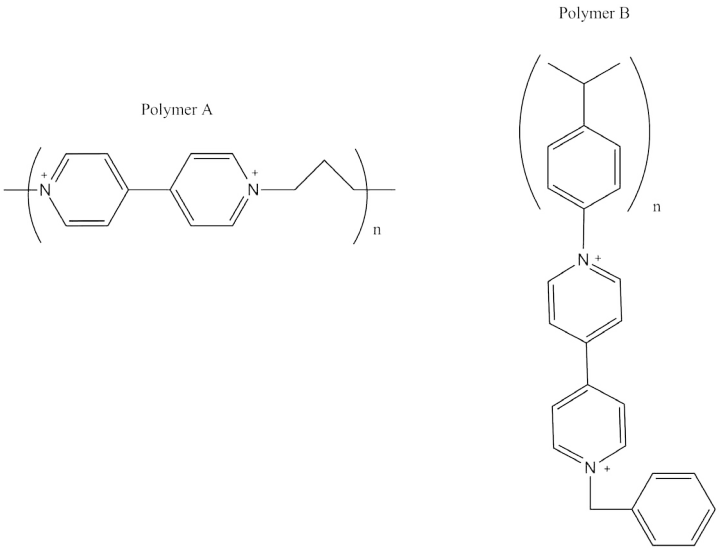

Figure 2.7 Soluble viologen polymers reported in Ref [3]. Polymer A is in-chain polymerized trimethylene viologens; polymer B is benzyl viologen appended to a polystyrene chain.

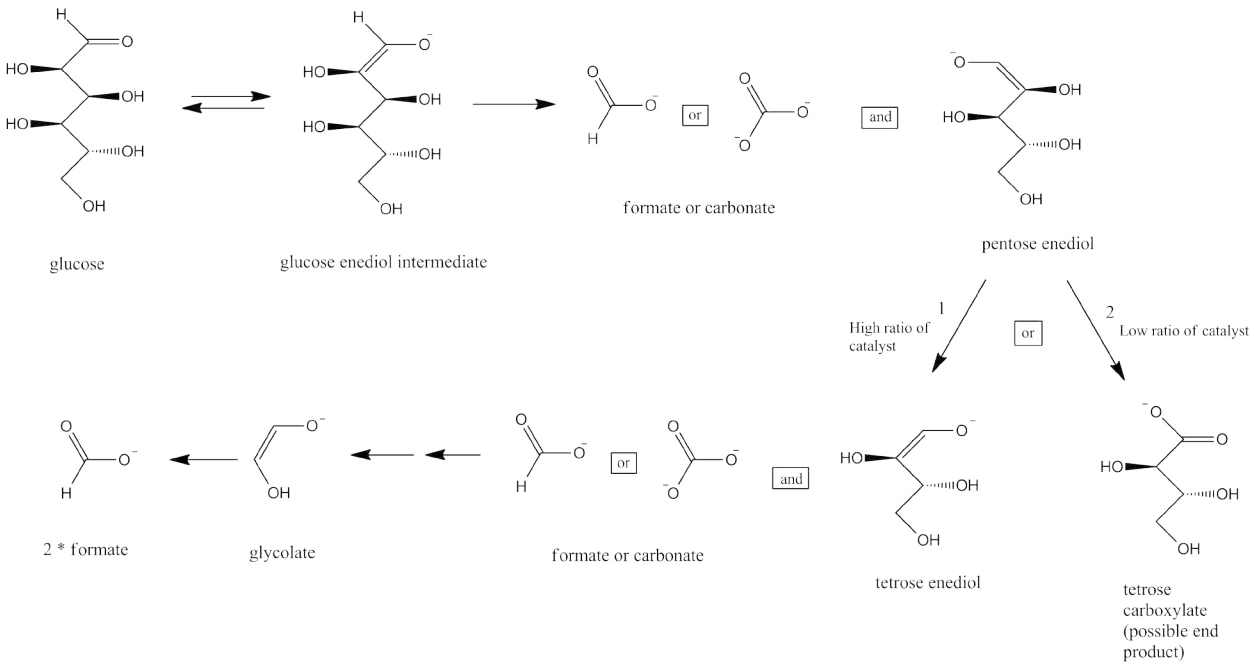

Figure 2.8 Proposed glucose oxidation mechanism [3].

Earlier research also found that not all carbohydrates are able to be oxidized by viologens. The ones that can appreciably react with viologen share one common characteristic: they all have a free anomeric carbon. Moreover, prior results also showed that the size of the carbohydrate monomer affected reaction rate. For instance, 6-carbon carbohydrates, like glucose, reacted more slowly that 5-carbon carbohydrate, with 3-carbon carbohydrates and analogues like dihydroxy acetone (DHA) reacting the fastest [3].

2.6 Viologen Polymers

The goal of the current work is based on the idea that immobilizes a novel viologen polymer onto an electrode surface; therefore it is essential to give a brief summary of some of existing viologen-derivative polymers and their applications along with the limitations to be employed in our DCFC system. The prior results demonstrated that carbohydrates can be catalytically oxidized by multiple viologens and that the oxidization efficiency increases with increasing viologen-to-carbohydrates ratios [3]. Watt and co-workers also showed that viologen polymers is a promising approach to provide a high localized catalyst concentration and simulate high viologen-to-carbohydrate ratios by minimizing the secondary reaction forming unreactive intermediates. Furthermore, Chapter 1 explains the importance of immobilization of viologens onto an electrode surface to make a practical and inexpensive DCFC devise. Generally speaking, there are two categories to consider: one where the viologen moieties are part of a polymer backbone and one where the viologen moieties are part of a pendant or side chain.

2.6.1 Viologen Moieties as Part of Polymer Backbone

In the first category, there are a number of reported studies. The first known case would be the viologen polymer made by Menschutkin reaction in 1974 with dihaloarylalkane or

dihaloalkanes and 4,4'-dipyridine [38]. Later in 1975 Simon and Moore made N, N'-bis-(aminoalkyl)-4,4'-dipyridinium polymer salts that are potentially of use as variable light filtering materials [39]. Endo and co-workers described the synthesis of polyethers containing viologen moieties by reacting tosylated polyethers with bipyridine, which acts an electron-transfer catalyst in organic reduction [40]. Osawa et al. and Leonida et al. reported the synthesis of electrochemically crosslinked polybutylviologen with glutaradehyde and co-electropolymerization of polybutylviologen and glutaradehyde, respectively, on a glassy carbon electrode [41]. The former authors reported on the use of the polymer for adsorption of diaphorase and the latter reported on use for conversion of NAD+ to NADH. More recently, Jain et al. incorporated viologens into polysilsesquioxane nanoparticles for electrochromic displays [42], and Kim et al. doped cobaltocene with viologens to form an electron active layer in inverted polymer solar cells [2]. The above-mentioned studies showed that different polymers with viologen moieties as part of polymer backbone have been widely used, and they can be potentially adapted as the viologen polymer for immobilization for this work.

2.6.2 Viologen Moieties as Part of Pendent or Side Chain

The second category of viologen polymer in which viologen moieties are part of pendant or side chain, also has been reported previously. Inaba et al. incorporated viologen into Nafion in solid polymer electrolyte composite electrodes as phase transfer mediators [43]. Sato and Tamamura prepared a polystyrene-type polyviologen, in which alkyl viologen moieties are hanging on the polystyrene backbone [37]. Similarly, Yamaguchi and Asano reported the synthesis of polypyrrole conductive polymer film with viologen side groups [44] and Yamaguchi et al. and Zhao et al. used viologen moieties as dopants to react with polyaniline [45, 46]. Song and colleagues introduced the preparation of polysiloxane viologen polymer with viologens as

side chain, reacting 1-methyl-1'–aminopropyl-4,4'bipyridinium salt with 3-aminopropyltrimethoxysilane. The resulting polymer was used to electrocatalytically reduce NAD+ and oxidize NADH [47]. Katz et al. added viologen moieties in the form of aminopropyl viologen to electropolymerized poly (acrylic acid) backbone on a gold electrode [48]. Very recently, as mentioned at the beginning of Section 2.5, Watt and co-workers [3] synthesized a film of polymeric viologen, made of benzyl viologen or phenyl viologen appended to polystyrene chain and attached it onto benzyl- or methyl- bromide activated graphite improve the carbohydrate oxidation efficiency for our DCFC. The aforementioned polymers are another form of viologen polymers that can be possibly used for immobilization in this work.

2.6.3 Discussion

We consider the prior work on polymeric viologens as candidates or our fuel cell anode. However, they all have some drawbacks in the context of our particular direct carbohydrate fuel cell.

The viologen polymers made via Menschutkin reaction are difficult to be tethered directly on metal surface or graphite and at least were not reported in known cases. Due to the nature of the afore-cited viologen polymers that are used in biological systems, they are specifically designed for certain substrates and not designed to work in alkaline conditions. Likewise, Nafion-corporated viologen polymers cannot function in high pH environment.

It would be more attractive to use viologen-containing conductive polymers, like polypyrrole and polyaniline, in our carbohydrate fuel cell, because the electrons transferred from carbohydrates to the viologens can be more efficiently passed onto the electrode in the present of the electron conductive backbone. However, the conductive backbone will generally undergo an irreversible deterioration of their π- conjugation in an alkaline environment [49].

Another promising approach is the one conducted by Katz et al. [48], adding the viologen groups on electropolymerized poly (acrylic acid) backbone on gold surface. The downside of this method is that polymerization of poly (acrylic acid) backbone on electrode surface may restrain the future development of introducing another monomer group to form co-polymeric viologen film.

Despite the fact that Watt's study showed some promising results to use viologens in their polymeric form to enhance carbohydrate oxidation efficiency, the selected viologen polymers in the study are not well suited for making a highly efficient fuel cell as they were shown to have a poor solubility and diffusion limitation because of their bulky structure, resulting in a slower interaction with the electrode than their corresponding monomers.

In summary, there have been a variety of viologen polymers developed and used in different areas. However, most of them are for electrochromic displays or biosensors. In both cases, efficiency and large current are not needed. In addition, some of the polymers are not designed for alkaline conditions, or some of them are more challenging to directly attach on metal surface or graphite surface.

2.7 Experimental

This section summarizes the electrochemical test devices and methods that are employed in this work and the related terminology of electroanalytical chemistry. Refs [50-52] are the main sources on which the information is based on. Other non-electrochemical methods used in this work include scanning microscopy (SEM), nuclear magnetic resonance (NMR) spectroscopy, mass spectroscopy, and X-ray photoelectron spectroscopy (XPS). These are discussed in Chapter 3.

2.7.1 Electrochemical Test Devices and Methods

Test devices: The electrochemical test device used in this work is a three-electrode cell, which is made of a working electrode, counter electrode and reference electrode. The working electrode is where the reaction of interest occurs. It can be the anode or cathode depending on direction of current flow. The anode is where the oxidation reaction (losing electrons) takes place and the cathode is where reduction reaction (receiving electrons) happens. Therefore, outside the electrolyte of the cell, the electrons are flowing from the anode to the cathode, and in the electrolyte, the ions are carried from the cathode to the anode.

The counter electrode is the auxiliary electrode where a complementary reaction takes place to the reaction happening on the working electrode. For example, if an oxidation reaction is happening on the working electrode, the cathode must carry out reduction reaction and vice versa. The counter electrode is usually made of inert or precious metal, such as platinum, that is not itself reactive so as not to interfere with the working electrode reaction; and it must have high surface area in order not be the location of a limiting current that can hinder the current at the working electrode. The counter electrode is not measured relative to the reference electrode and the reaction happening at the counter electrode is of less concern so long as the product of the reaction does not interfere with the reaction at the working electrode.

The reference electrode serves to measure the potential of the working electrode of an electrochemical cell. The measured potential is relative to the thermodynamic, well-known, and stable equilibrium potential of the reference electrode. There are many types of reference electrodes that are used, the most common laboratory reference electrodes are the saturated calomel electrode (SCE) and the silver-silver chloride electrodes. Their potentials can be given with respect to the standard hydrogen electrode (SHE). The reference potential is dependent on

the concentration of the ions that participate in the redox reaction at the reference electrode. Technically, one needs to correct the measured reference potential, depending on the concentration change in the liquid junction between the main cell and the solution inside the reference electrode compartment. However, this potential change is typically only on the order of mV, and it is not taken account in this work. Throughout the electrochemical experiments in this work, a silver-silver chloride reference electrode is used and KCl is used as a supporting electrolyte in each cell. The silver-silver chloride reference electrode is made in-house and details of the experimental fabrication procedure are discussed in Chapter 4 and 5.

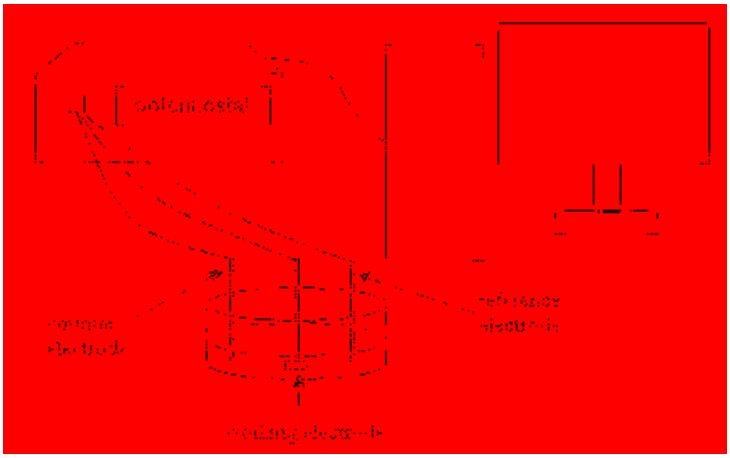

Figure 2.9 Scheme of a three-electrode cell set-up connected to a computer.

Test methods: Figure 2.9 shows a diagram of a potentiostat, an electrochemical instrument, which is connected with the three-electrode cell. In a potentiostat, an external power source is used to impose certain potential or current on a cell. The potentiostat can be used for different types of electrochemical experiments, such as potentiostatic and voltammetric experiments. For a potentiostatic experiment, the resulting current is detected and measured when the potential between the working and reference electrodes is kept static. In voltammetric

experiments, e.g. cyclic voltammetry, the potential at the working electrode is linearly swept verses time in the form of a triangle wave, and repeated for multiple cycles. The resulting current profile is recorded between the working electrode and counter electrode [53].

Cyclic voltammetry (CV) is a popular electrochemical analysis technique and has been proven useful in obtaining information for fairly complicated electrode reactions. But CV is limited to static systems, where there is no flow at the electrode surface; it is not a reliable method to obtain transport and kinetic variables for a hydrodynamic system, where flow is achieved at the electrode surface by stirring, pumping or rotating the solution [50].

A rotating disk electrode (RDE) system is a valuable experimental tool that is easy to set up and allows us to study the effects that convection and diffusion have on chemical reactions. RDE is particularly good at determining surface kinetics because of its capability of controlling the transport regime of electroactive species toward the electrode [54]. On the other hand, the downside of RDE is the possibility for turbulent flow, which violates assumptions used to analyze the experiment. RDE method was employed in Chapter 5 in this work; the intention to use RDE here was for purpose of stirring.

Figure 2.10 (a) and (b) shows a schematic representation of a typical RDE. The electrode itself is a flat, circular disc of graphite or metal or any other conductor. The disc is embedded centrally into one flat end of a cylinder, which is made of insulator material, such as Teflon or epoxy resin. The distance between the electrode and the edge of the insulator cylinder shaft is 5-8 mm; this additional distance is needed in order to minimize the effects of eddy currents [50]. Behind the face of the electrode is an electrical connection leading to the potentiostat that controls the potential of the electrode. The set-up of a rotating disk electrode (RDE) continues to be a three-electrode cell, with the RDE as the working electrode. During the course of

experiments, the RDE is immersed in the solution of analyte, with the face of the disc immersed. The disc is spun at a fixed, known frequency about its central axis and the current through the disc is then measured as a function of the potential applied and rotation speed ω.

Figure 2.10 (c) is a schematic diagram that shows the direction of solution flow over the face of the RDE during rotation of the electrode. As the electrode rotates, the solution is dragged by the spinning disk towards the electrode face, and the resulting centrifugal force flings the solution away from the center of the electrode, out towards the rim of the cylinder. Movement of solution away from the disc center causes more solution to be drawn from the bulk solution towards the electrode face. The end result is a form of laminar flow, and the rate of the solution flow can be controlled by the electrode's angular velocity. At very high rates, this convective flow can achieve conditions in which the steady-state current is controlled by surface kinetics rather than by diffusion.

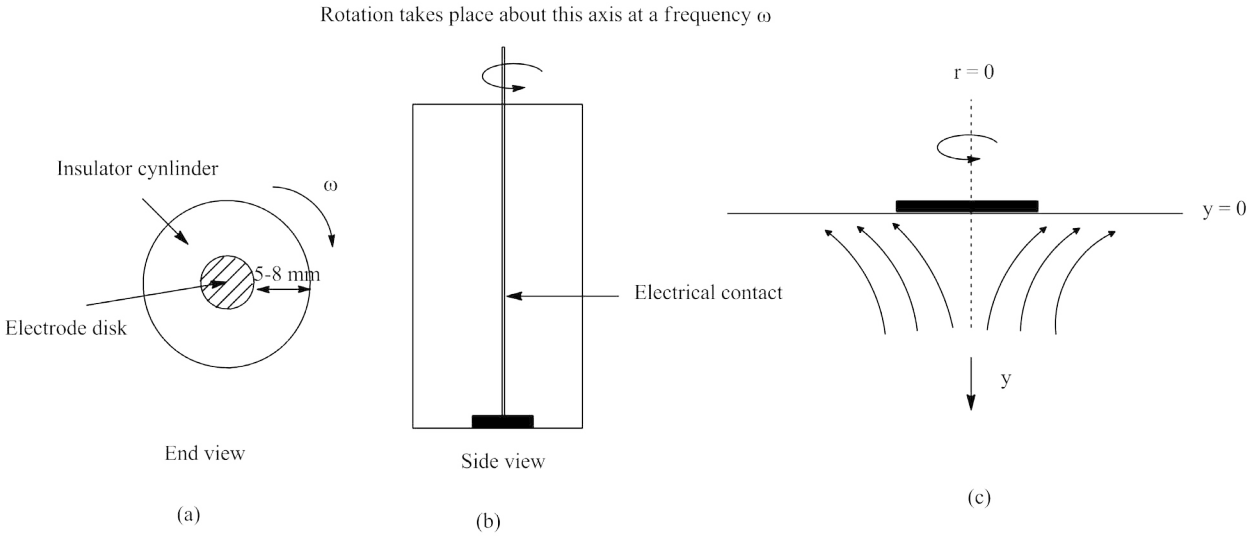

Figure 2.10 (a) and (b) are schematic representation of a rotated disk electrode (RDE); (c) is schematic representation of the direction of the solution flow over the electrode face.

Another electrochemical method in this work is the use of a lab-scale fuel cell. Figure 2.11 shows a schematic diagram of this fuel cell, which was modified from a small methanol demonstration fuel cell that is commercially available. The apparatus has a closed compartment for the anode and has an air cathode. A plastic bag covers the anode compartment and is used to create a nitrogen blanket to exclude air. The anode is composed of the anode compartment and a nickel foam (Marketech International, USA) that is the current collector. The reference electrode is placed in contact with the fluid in the anode compartment. The anode and cathode plates are stainless steel. The cathode material is E-5 cobalt-based carbon cathode (electric-fuel.com). The separator is an ion-exchange membrane that allows ions go through but keep O_2 on the cathode side. The ion-exchange used in work is an anion-exchange membrane, which was purchased from Tokuyama Corp, Japan, A201(OH) and Lot A-0033. This apparatus is a three-electrode cell, and connected with a potentiostat. The anode is the working electrode and the cathode is the counter electrodes, which are connected to the potentiostat accordingly.

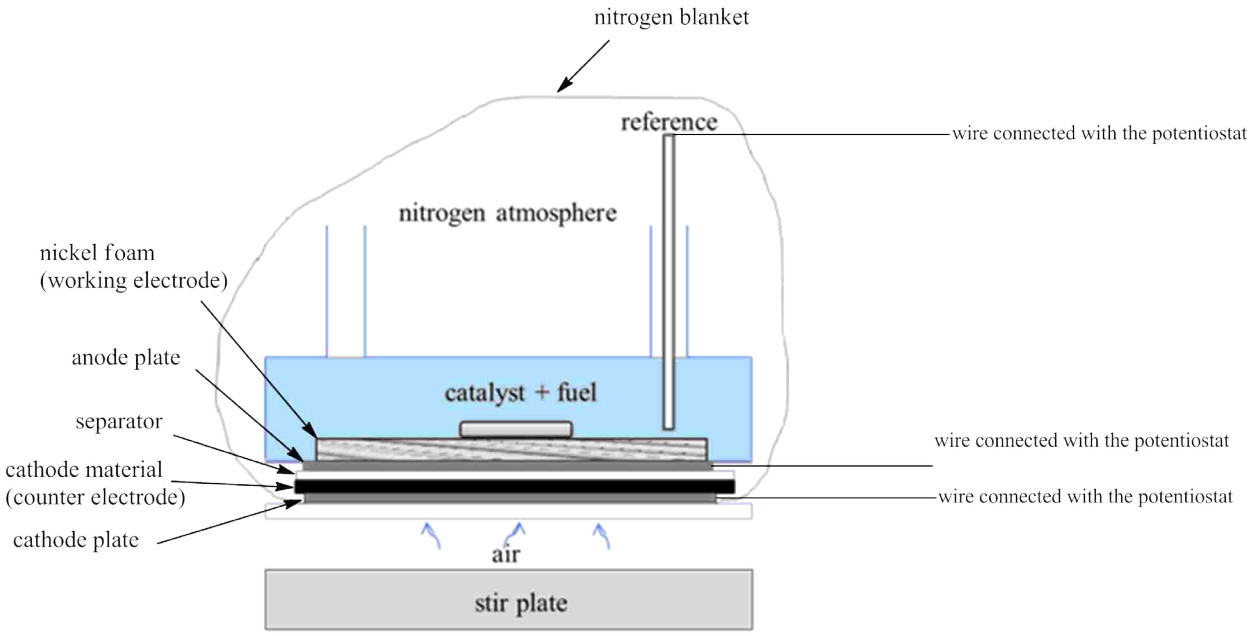

Figure 2.11 Schematic of the modified small methanol demonstration fuel cell used in this work [20].

2.8 Conclusion

Glucose and other carbohydrates molecules are among the most abundant and renewable energy sources in the world, and potentially can be used as alternative fuels to supplement fossil fuels. Prior results have shown that viologens are effective catalysts for oxidizing these molecules for use in a direct carbohydrate fuel cell. Monosubstituted viologens were shown to be more suitable catalysts for use in our fuel cells to catalytically oxidize carbohydrates. This is because monosubstituted viologens are more stable in high pH conditions and have more favorable redox potentials compared with their analogous disubstituted viologens. All the tested homogenous viologens are orally toxic to humans and must be immobilized onto an electrode surface. Moreover, prior work has shown that there is a need for high ratios of catalyst to fuel in order to prevent formation of an unreactive intermediate product. Viologen polymer appears to be a way to fulfill this need by increasing local concentration of viologens.

3 Synthesis and Analysis of Two New Types of Viologen Molecules and the Novel Viologen Monomer

3.1 Introduction

This chapter includes synthesis and analysis of two new viologen molecules and of a novel viologen monomer. The two viologen molecules were used to investigate the diffusivity and electrochemical activity for mono- and di-substituted viologens. The novel viologen monomer is synthesized for the intention of immobilization. As stated in Chapter 1, viologens are orally toxic to humans and must be immobilized onto a surface to make a practical fuel cell device.

The reader may wonder why this work includes the synthesis of the two new viologen molecules that are not related to the immobilization objective. Part of the reason was to assist another parallel study on carbohydrate fuel cells. Also, the development of the synthesis for these two molecules provided a training experience in preparation for synthesizing the novel viologen monomer.

Molecules: The two new viologen molecules reported here are methylaminopropyl viologen (MAV) and aminopropyl viologen (APV). The corresponding molecular structures are shown in Figure 3.1. Prior work has shown that mono- and di-substituted viologens, in the form of monoalkyl and dialkyl viologens, have different catalytic performances toward carbohydrates oxidation, and monoalkyl viologens appeared to be a more suitable catalyst for use in our fuel

cells [20]. To better understand the suitability of monosubstituted viologens, an electrochemical comparison of a series of monoalkyl and dialkyl viologens was carried out through cyclic voltammetry (CV) tests, where the variation in the redox potential as the length of the alkyl chain changed was assessed. Among the tested viologens, MAV was used as one of the dialkyl viologens, and APV was used one of the monoalkyl viologens [21].

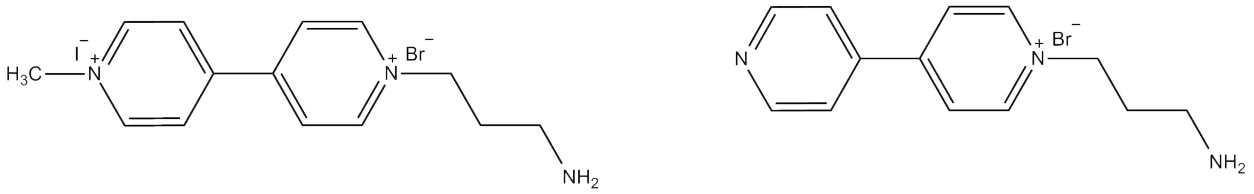

Methylaminopropyl viologen (MAV)

Aminopropyl viologen (APV)

Figure 3.1 Images of molecular structures of methylaminopropyl viologen (MAV) and aminopropyl viologen (APV).

Prior results showed that there is a need of utilizing of polymeric viologens to increase the local concentration of catalyst in order to prevent formation of unreactive intermediate product during the glucose oxidation [3]. The novel viologen monomer developed in this work, 1-(3-acrylamidopropyl)-[4,4'-bipyridin]-1-ium bromide (AAPB), is shown in Figure 3.2. This particular structure was chosen mainly for two reasons. First of all, AAPB is a monosubstituted viologen. As guided by the prior results included in Chapter 2, monosubstituted viologens were shown to be more suitable catalysts for use in our fuel cells than their analogous disubstituted viologens, as they are more stable in high pH conditions and have more favorable redox potentials. A second reason for our choice of monomer is that the alkyl chain between the viologen moieties and the terminal acrylamide group is flexible and capable of withstanding high

pH. The alkyl chain would allow the viologen moieties to achieve an appropriate steric alignment with carbohydrate molecules in solution, and efficiently transfer electrons from carbohydrates to the anode.

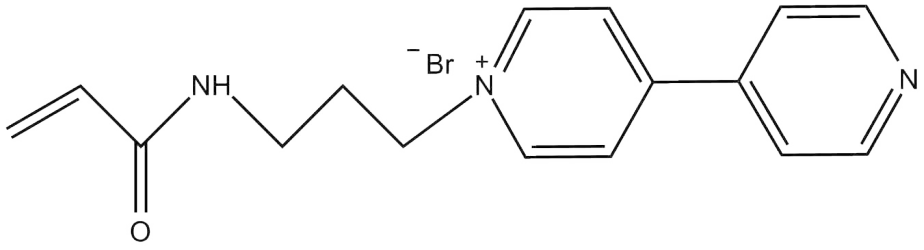

1-(3-acrylamidopropyl)-[4,4'-bipyridin]-1-ium bromide

Figure 3.2 Image of the novel viologen monomer (AAPB).

3.2 Experimental Methods and Materials

3.2.1 Materials

4,4-dipyridyl, 3-bromopropylamine ·HBr mixture, acryloyl chloride, iodomethane, acetone, hydroquinone, acetonitrile and were purchased from Sigma Aldrich and used without purification. Chloroform, NaOH (in the form of pellets) and dichloromethane were purchased from Mallinckrodt. Methanol and H_2SO_4 were supplied by Macron. NaCl and Na_2SO_4 were purchased from Fisher Scientific. All solvents, including acetone, acetonitrile, chloroform, dichloromethane, and methanol were the reagent grade. Sodium bicarbonate (baking soda, Arm&Hammer) was used as received. All aqueous solutions were made with double-distilled water. Thin-layer chromatography plates are silica on aluminum foils that were purchase from Sigma-Aldrich. Micro pipets (10μL) used for spotting TLC plates were supplied from VWR.

3.2.2 Synthesis

Methylaminopropyl viologen (MAV): The synthesis approach is a modification of the method carried out by Katz et al. [48]. There are two steps to prepare MAV, N-methyl-N'-(3-aminopropyl)-4,4'-bipyridinium. The synthetic pathway is shown in Figure 3.3.

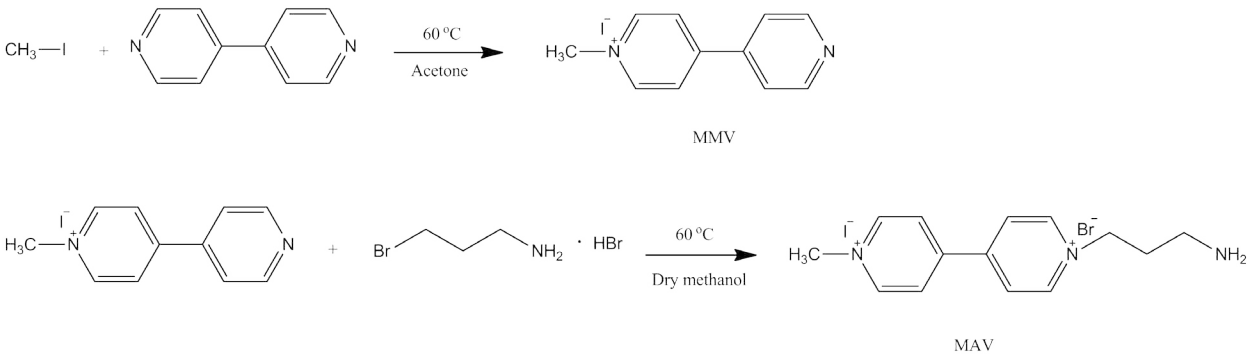

Figure 3.3 Synthetic pathways for making MAV.

In the first step, 1-methyl-4-(4'-pyridyl)-pyridinium iodide (monomethyl viologen, MMV) was formed by reaction of iodomethane and 4,4'-bipyridine. 1.92 g of 4,4'-bipyridine was dissolved in 20 mL of acetone in a three-neck flask. Subsequently, 1.76 mL of iodomethane was added dropwise while the mixture of 4,4'-bipyridine and acetone was magnetically stirred. The reaction was stirred at 60 ºC for 8 hours under nitrogen and water-cooled reflux. Monomethyl viologen (MMV) was produced in the form of an orange precipitate, which was then filtered and washed with acetone several times to remove the residual unreacted 4,4'-bipyridine. At the end of the first step, 3.35 g of MMV was formed and ready for the next step. The yield was 69 mol %.

In the second step, 25 mL of dry methanol was used as solvent, in which 3.35 g of MMV and 4.26 g of bromopropylamine ·HBr mixture were placed. The reaction mixture was stirred for

48 hours under nitrogen and water-cooled reflux at 60 ºC. The final product was orange precipitate, which was then filtered and washed with pure ethanol. The yield was 1 g (12 mol %) of pure MAV. The composition and purity were verified by NMR spectroscopy.

Aminopropyl viologen (APV): APV, N-(3-aminopropyl)-4,4'-bipyridium, was obtained through a one-step reaction synthesis and the synthesis was developed in-house. 0.219 g of bromopropylamine + HBr and 0.468 g of 4,4'-bipyridine were added to 20 mL of dry acetonitrile. The reaction was run for 48 hours at 75 ºC with stirring under nitrogen and water-cooled reflux. A white product precipitated from the reaction mixture; it was then filtered and washed with dry acetonitrile to eliminate any unreacted reactants. The product was effectively 100% yield with 0.293 g of APV. The composition and purity were verified by NMR spectroscopy.

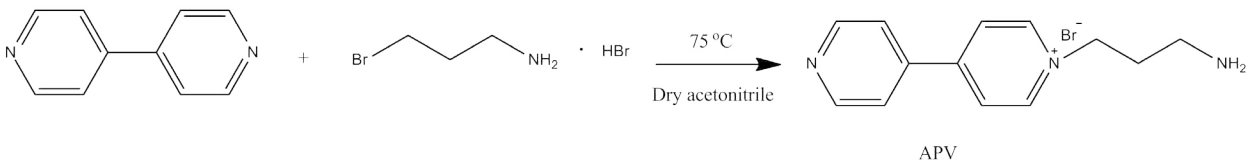

APV

Figure 3.4 Synthetic pathway for making APV.

Novel viologen monomer (AAPB): There are two steps for the synthesis of the AAPB monomer. The synthetic approach was adapted from the work done by Bibart et al [55]. The reaction pathway was developed in-house, and is shown in Figure 3.5.

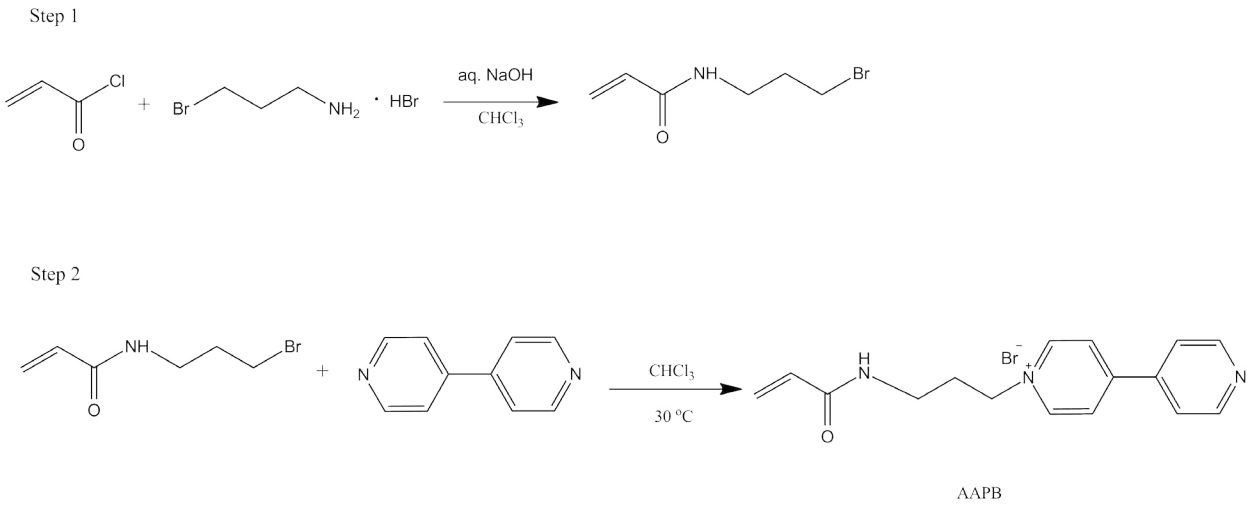

Figure 3.5 Synthetic pathways for making AAPB monomer.

For step 1, 0.5 g of NaOH was dissolved in 10 mL of water and 0.438 g of 3-bromopropylamine (BPA) ·HBr mixture was added to the solution in a round-bottom flask. NaOH is used to deprotonate BPA and makes the amine group available to react with the acid chloride. Then 13 mL of chloroform was added. In a separate container a solution containing 0.48 mL of acryloyl chloride was added to 2 mL of chloroform in an ice bath. This second solution was added dropwise to the bottom chloroform phase of the first solution by inserting a pipette into the lower phase while the mixture was kept on ice. The resulting solution was reacted overnight with stirring and under an N_2 atmosphere in an ice bath. The aqueous phase was then removed by pipetting and the chloroform phase was washed sequentially with 10 mL of 1 M H_2SO_4, 10 mL of 1 M $NaHCO_3$ solution, and 10 mL of a saturated NaCl solution. These washes were done separately and sequentially with removal of the aqueous residual phase between each washing. Finally the chloroform phase was dried with excess Na_2SO_4 that was then removed. Reduction of cloudiness indicated the aqueous phase was substantially removed. This concluded step 1 to create the intermediate monomer.

In the second synthesis step, 0.924 g of 4, 4-dipyridyl was dissolved in 5 mL of chloroform, which was then added to the layer of dried intermediate compound from the first step. This was transferred to a clean flask. A tiny amount of hydroquinone (4 ppm) was also added to prevent the polymerization during the reaction. The mixture was stirred and reacted under an N_2 atmosphere at 30 ºC and water-cooled reflux for two days. The raw monomer product is a yellow/brown, sticky and somewhat oily precipitate that is not soluble in chloroform or acetone. After the reaction period, the chloroform solution was poured out of the reaction flask, leaving the solid product behind. Because the monomers are sensitive to temperature, it is necessary to refrigerate the formed product promptly to minimize polymerization. The raw monomer product was then washed thoroughly with chloroform and then with acetone to remove any unreacted reactants. Before washing with acetone, the chloroform was removed by pipetting. As acetone is highly volatile and miscible with chloroform, the washed raw product was almost solvent-free after removal of acetone. The raw product was then dissolved in methanol and stored in a refrigerator at 2 – 4 ^{o}C for as long as 1 week prior to the next separation step. About 0.1 – 0.15 g of raw monomer product can be made in total per batch. This is a yield of about 15 % to 22 %.

AAPB monomer was purified from the raw monomer product by column separation. The column was filled with silica gel (200-300 mesh) in dichloromethane; the elution solvent was made of 1 equivalent methanol and 2 equivalents dichloromethane. The dimension of the column used in this work is showing in Figure 3.6.

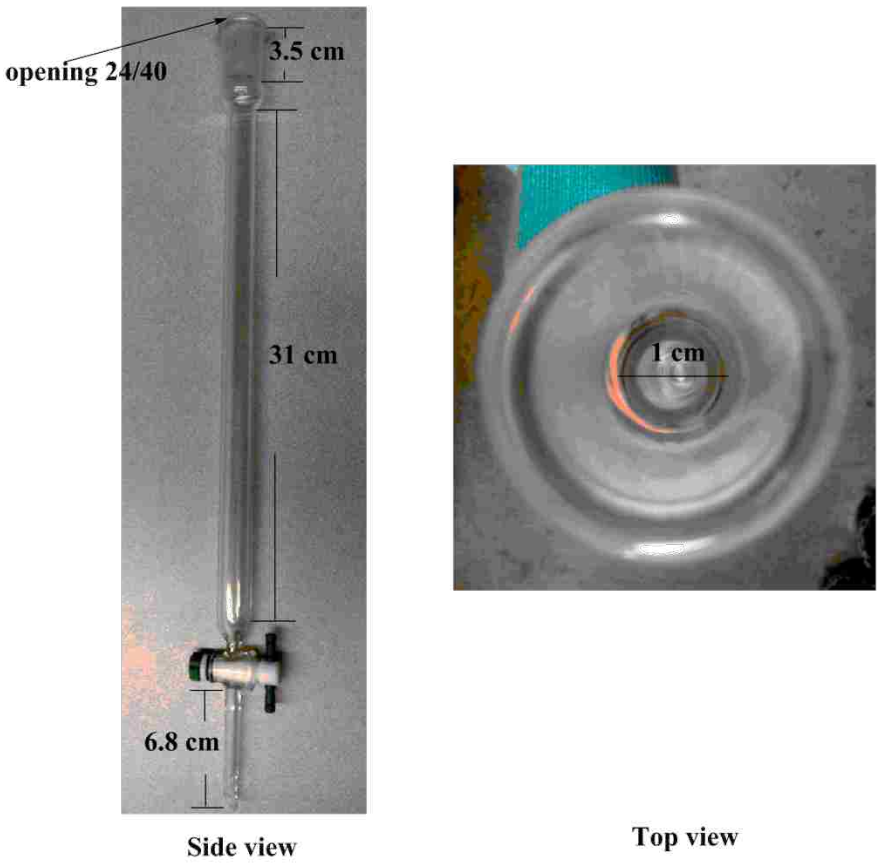

Figure 3.6 Dimensions of the column.

Just enough cotton was inserted at the bottom of the column to prevent any leaking of the silica gel. About 20 mL of silica gel dissolved in 40 mL of dichloromethane and added to the column slowly while keeping the valve at the bottom of the column closed. The silica gel was then stirred with a metal wire that is long enough to reach the bottom of the column to eliminate any trapped air bubbles. After stirring, the added silica gel was allowed to settle while opening the valve and letting the solvent, dichloromethane, drain slowly. The level of the dichloromethane was kept above the silica gel all times. At the point when the silica gel was no longer moving and dichloromethane was 1 cm above this layer, then about 1 cm thickness of sand was added to act as a physical barrier. During the course of experimentation, 1.3 g of raw

product was found to be a reasonable amount of material to be separated for 20 mL of silica gel. The raw product stored in methanol was added slowly into the column using a pipette. At the same time, a series of test tubes were used to collect the eluent samples. After the entire raw product flowed into the silica gel, the eluent solvent made of 1:2 methanol and dichloromethane by volume was slowly run into the column.

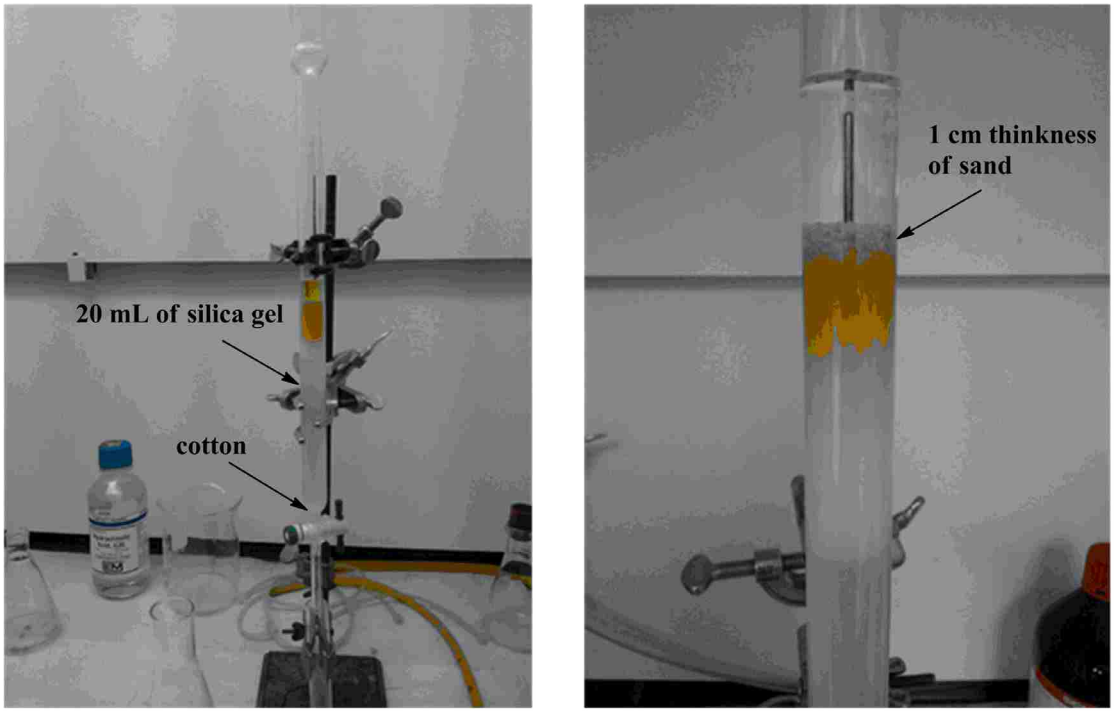

Figure 3.7 Demonstration of column separation set-up discussed here.

When the column separation step was completed by collecting enough eluent samples, thin-layer chromatography (TLC) was employed to identify the pure monomer. A micro pipet (10μL) was used to deposit an eluent sample on a TLC plate. Figure 3.8 shows a developing chamber containing a TLC plate. The spotted TLC plate was then placed in the closed chamber with developing solvent made of 1:10 methanol and dichloromethane by volume (see Figure 3.8). The plate was removed from the developing chamber when the solvent front is 1-1.5 cm

from the top of the plate. The plate was visualized by exposure to ultraviolet light. Detailed TLC procedure can be found in Ref [56].

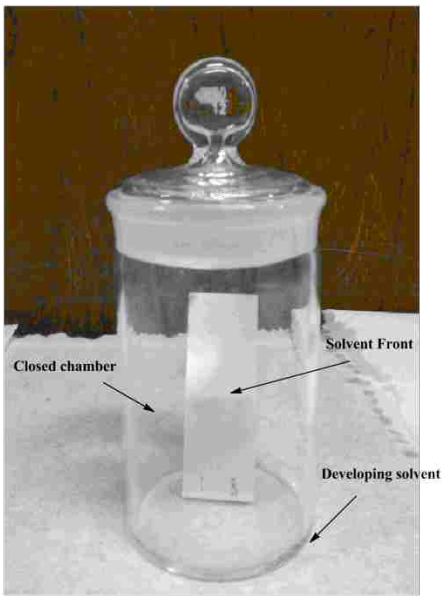

Figure 3.8 Developing chamber containing a TLC plate.

Figure 3.9 shows a series of TLC plates, each corresponding to a separate eluent sample. The marked circles represent where the sample material traveled to in the developing solvent when exposing to ultraviolet light. It was found that for the first couple of sample tubes, part of the sample material traveled to the middle of the TLC plate, which indicates impurity. Once the sample material remained completely at the bottom of the TLC plate, it means the pure monomer was present in the corresponding eluent. When the middle spot showed up again on later the TLC plate that means pure monomer was running out and impurities were again present.

The eluent for the successful (relatively pure monomer) samples was then combined and solvent was evaporated in air to dryness. The collected pure AAPB monomer was then verified by NMR spectrometry and mass spectrometry; the analysis is included in Section 3.3. One

column fed with 1.3 g raw reaction product yielded 0.04 g of high-quality nearly pure (90%) monomer.

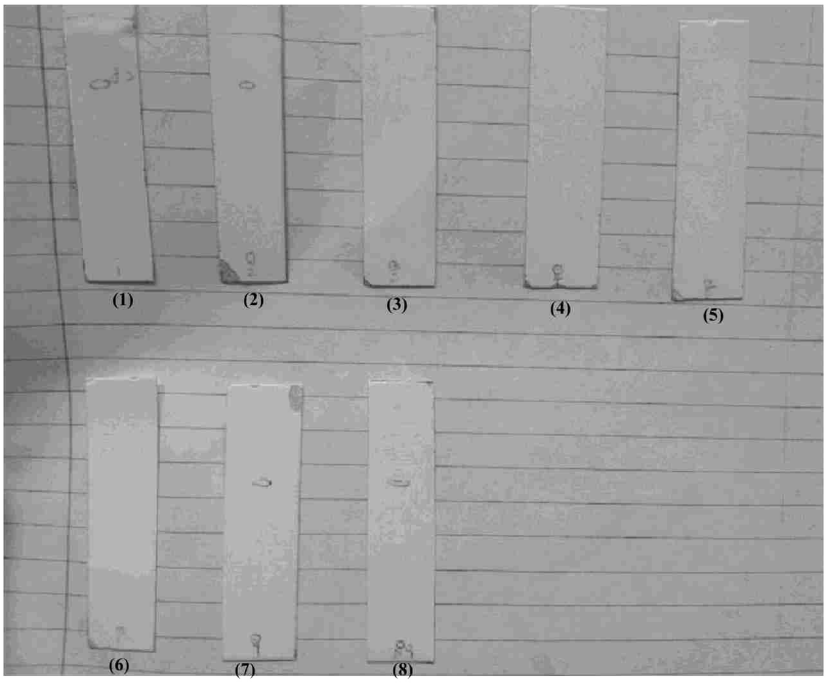

Figure 3.9 Demonstration of the resulting TLC plates.

3.3 Results and Discussion

Methylaminopropyl viologen (MAV): Figure 3.10 shows the ^{1}H NMR spectrum of MAV in D_2O, including peak assignments. The peak corresponding to the N-methyl group is labeled at position 1, namely 4.4 ppm, and integrates to 3 hydrogens. The hydrogens on the bipyridinium ring are located at positions 2, 3, 4 and 5, which shift at 9.1 ppm, 8.9 ppm, 8.5 ppm and 8.4 ppm respectively. Each of the peaks integrates to 2 hydrogens. The propyl chain, located at positions 6, 7, and 8 are shifted at 4.7 ppm, 2.4 ppm and 3.1 ppm respectively, and each peak integrates to 2 hydrogens. The hydrogen, located at position 9, at the terminal amine group is not

observed on the spectrum. The hydrogen on the amine can form a hydrogen bond with the oxygen in surrounded D_2O, and the hydrogen and deuterium are rapidly exchangeable [57]. In summary, all the peaks and corresponding integrations shown on the ^1H NMR spectrum conform well to the proposed structure of the MAV molecule.

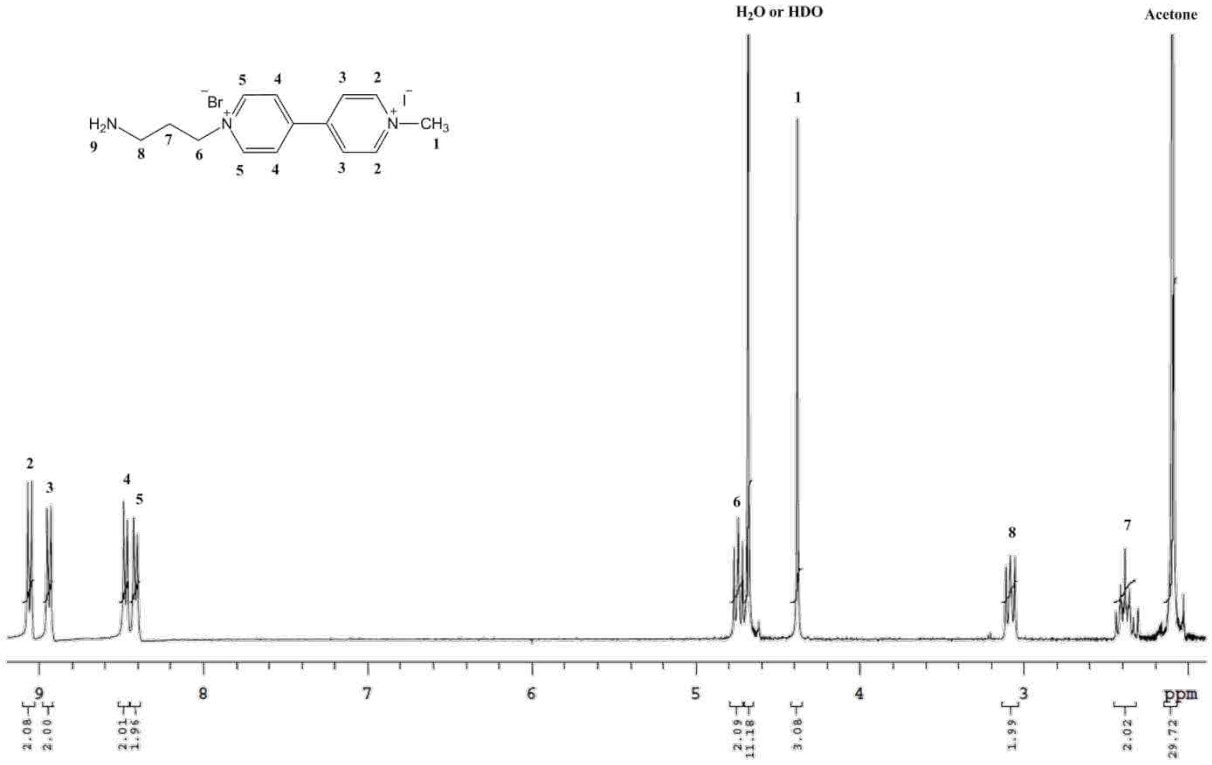

Figure 3.10 ^1H NMR spectrum of AAPB monomer in D_2O.

Aminopropyl viologen (APV): ^1H NMR spectroscopy is again used to verify the synthesis of APV. Figure 3.11 shows ^1H NMR spectrum of APV in D_2O. Peak assignments and integrations are shown in the figure. The peaks labeled positions 1, 2, 3, and 4 represent the hydrogens on the bipyridinium ring, and have shifts of 8.9 ppm, 8.7 ppm, 8.35 ppm and 7.8 ppm respectively. The signal corresponding to position 5 is obscured by H_2O or HDO peak (the rightmost peak of the triplet is what we can see). The peaks corresponding to positions 6 and 7

are labeled on the spectrum as shown, which are located at 2.38 ppm and 3.03 ppm respectively. The hydrogen at the end amine group is represented by position 8. Similarly, as discussed for the case of MAV, the hydrogen on the amine group is not observed because of the hydrogen bonding between the amine group and D_2O, and after the hydrogen is swapped with the D, the peak is not shown. The spectrum shows a tiny amount of unreacted 4,4'-bipyridine in the final product, but no detectable trace of disubstituted viologen, meaning the viologen produced is nearly pure monosubstituted APV.

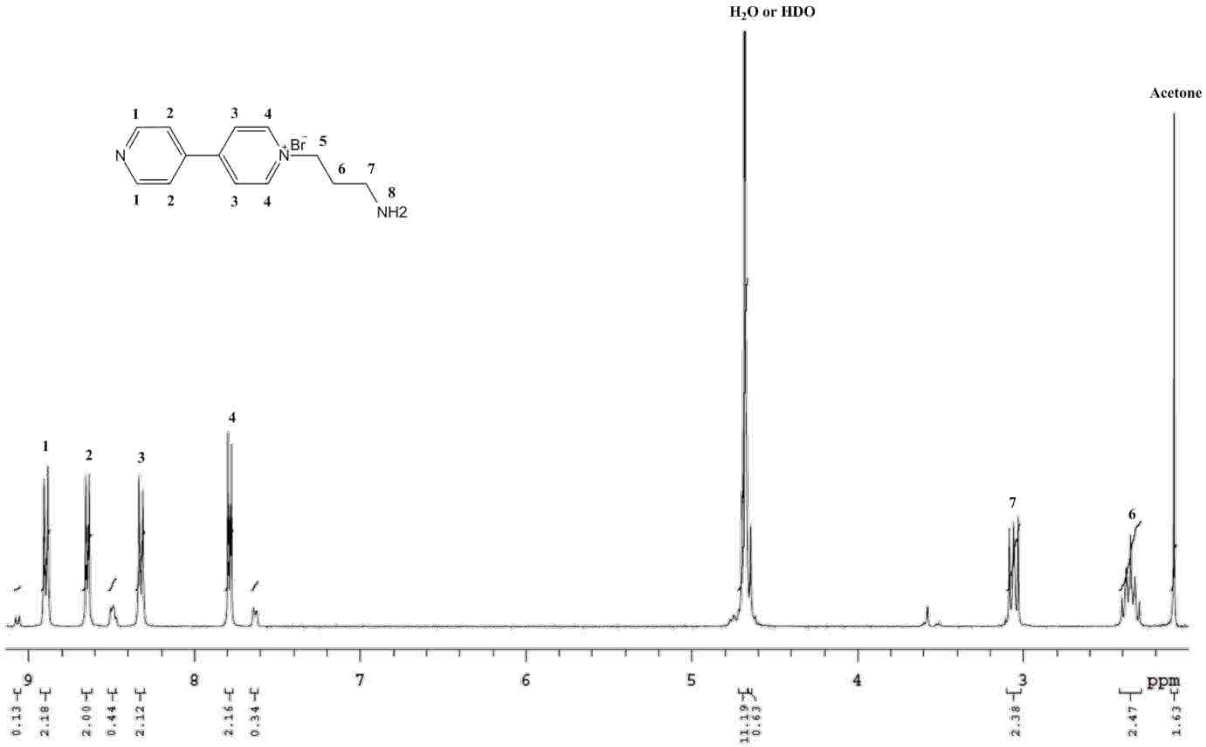

Figure 3.11 ^{1}H NMR spectrum of APV in D_2O.

Novel viologen monomer (AAPB): The synthesis of AAPB monomer was verified by ^{1}H NMR spectrometry and mass spectrometry. Figure 3.12 shows the ^{1}H NMR spectrum of AAPB monomer in D_2O. Peak assignments and integrations are shown in the figure. The peaks

corresponding to the bipyridinium ring are located at positions 1, 2, 3 and 4, which shift at 8.65 ppm, 7.8 ppm, 8.3 ppm and 8.9 ppm respectively. Each of the peaks integrates to 2 hydrogens, indicating good accord with the intended monomer compound. In the presence of the electron-withdrawing bipyridinium ring, the peaks corresponding to the propyl protons are shifted to higher magnetic field positions, namely 4.6 ppm, 2.26 and 3.3 ppm for position 5, 6 and 7, respectively, again with an integration of 2 hydrogens for each peak. However, the peak corresponding to the position 8 is not observed because the hydrogen on the amide can form hydrogen bonding with the oxygen in D_2O, and the hydrogen and deterium are exchangeable [57]. The peaks corresponding to the vinyl protons are labeled 9 and 10, shifting at 5.6 ppm and 6.1 ppm. Solvents peaks, namely, HDO and acetone, are also shown in the spectrum. It can be noticed that there is a small amount of impurity detected, corresponding to the unassigned peaks.

Figure 3.13 shows the mass spectrum of the AAPB monomer product. The huge peak shows the molecular weight of the AAPB monomer without Br^-, 268 g/mol. It further confirms the synthesis of the viologen monomer in the presence of a small quantity of impurities.

3.4 Conclusion

Methylaminopropyl viologen (MAV), aminopropyl viologen (APV) and the novel viologen (AAPB) monomer were synthesized and purified. The MAV and APV molecules were made through a 2-step and 1-step synthesis processes respectively, and were verified by ^1H NMR spectroscopy. Both MAV and APV were obtained at a high production yield. There was no trace of disubstituted viologen detected in the final APV product; however, a tiny amount of unreacted 4,4'-bipyridinie residual was found. AAPB monomer was made by a 2-step synthesis process,

and was then purified by a column separation process. Despite the low yield, the final AAPB monomer was obtained at 90 mol % or greater purity.

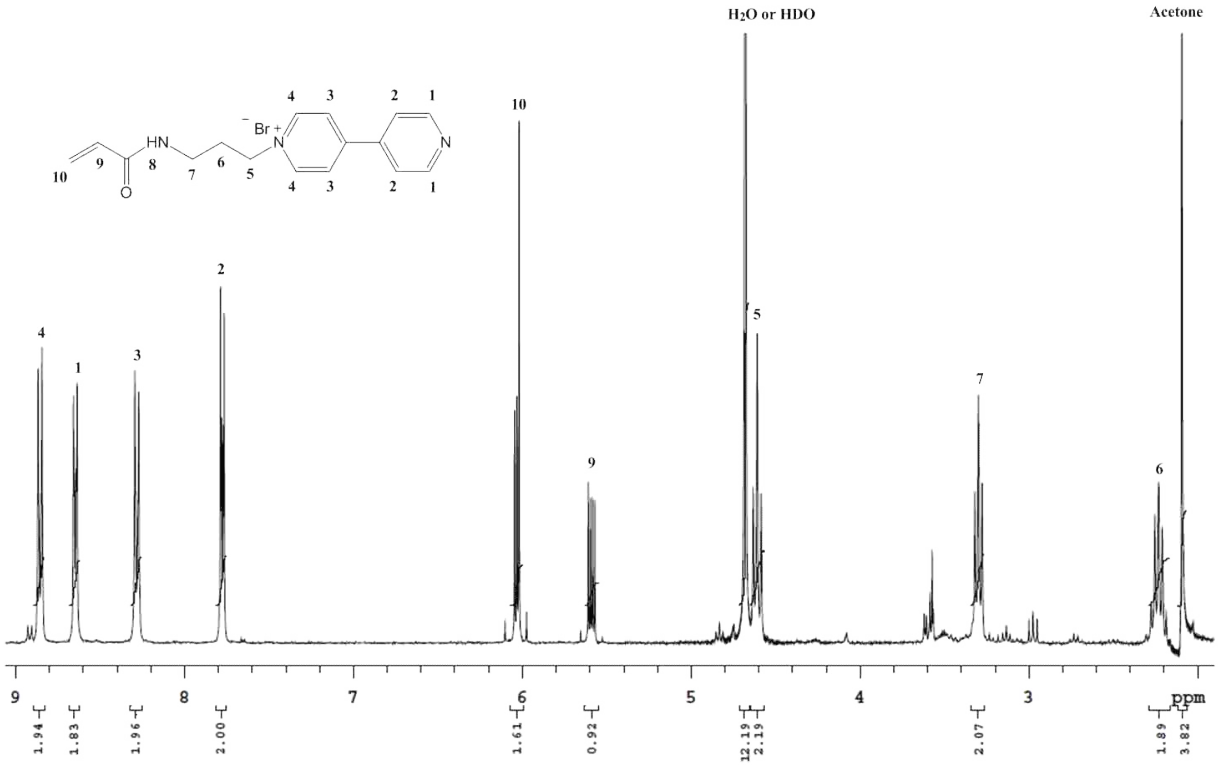

Figure 3.12 ^{1}H NMR spectrum of AAPB monomer in D_2O.

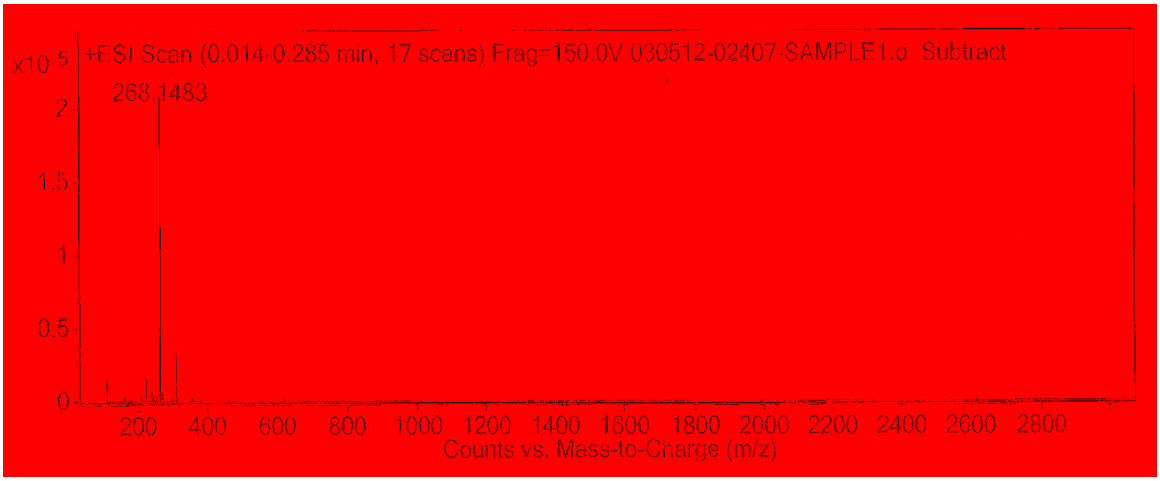

Figure 3.13 Mass spectrum of AAPB monomer.

4 Cyclic Voltammetry Investigation of the Synthesized Viologen Molecules

4.1 Introduction

This chapter discusses the electrochemical investigation of the methylaminopropyl viologen (MAV), aminopropyl viologen (APV) and the novel viologen (AAPB) monomer.

The electrochemical investigations in this chapter were carried out by cyclic voltammetry (CV). Cyclic voltammetry was used to study the electrochemical properties of MAV and APV, including diffusivities (D) and heterogeneous electron-transfer coefficients (k_{et}). The work presented here on MAV and APV were undertaken with collaboration with Dane Hansen, a former PhD student of BYU Chemical Engineering Department. In particular, the CV data concerning MAV and APV in Section 4.3 was produced by Hansen and previously published in Ref [21]. The present author synthesized these viologens as discussed in Chapter 3. The values of D and k_{et} included in this chapter were also revised by the present author; namely there was an improvement of the extrapolation procedure in Hansen's data reduction. For the electrochemical investigation of the AAPB monomer, cyclic voltammetry was used to examine the initial electrochemical activity of the AAPB monomers in their homogenous form. Because AAPB monomer was to be attached to an electrode surface as our intended application, electrochemical properties, like diffusivity (D), may become less important.

4.2 Experimental Methods

The cyclic voltammetry experiments were performed with a Gamry PC4/750 Potentiostat. The software used to analyze the CV data was the Gamry Echem Analyst version 1.10. The instrument has a precision range of about ±5 mV.

A three-electrode cell was used. The counter electrode was high-surface-area platinum gauze and the reference electrode was AgCl reference electrode, which was made by anodizing a silver wire in 1 M KCl at 2 V vs Ag/AgCl for 10 minutes. For CV tests in aqueous solution, the reference electrode solutions were made of 3 M KCl with saturated AgCl; for CV tests in DMSO, the reference electrode solution were made of 0.1 M TBACl (tetra-N-butylammonium chloride) in DMSO with saturated AgCl. The reference electrode tube was purchase from Microelectrode, Inc. After use each day, the reference electrode tube filled with the reference electrode solution was stored in a solution of saturated KCl and AgCl, and the reference electrode wire was stored in double-distilled water under dark. The reference electrode solution was changed daily and the reference electrode wire was refreshed regularly to ensure stability, using the above anodizing procedure.

The working electrode was a platinum disk (1.6 mm diameter). It was cleaned between runs by rinsing with 2 N nitric acid followed by double-distilled water. For the CV tests in DMSO, prior to the test the electrode was rinsed with water then acetone, dried and then rinsed twice with DMSO. After the final rinsing, the electrode was dried and polished on qualitative-grade filter paper (supplied from VWR) [50].

Figure 4.1 shows the apparatus setup for the CV experiments conducted in this chapter. For our tests, 10 mL of test solution was placed in a 30 mL glass jar. The lid to the jar had fitted holes for insertion of the electrodes and for nitrogen to be bubbled through the solution. The test

solution was further isolated from oxygen in the atmosphere by placing the jar in a resealable plastic bag. The electrolyte solution was purged of oxygen by bubbling solvent-saturated nitrogen into the cell for 15 minutes prior to initiating the electrochemical experiment. The nitrogen blanket was maintained over the test solution during tests. The flow rate of nitrogen was adjusted until no change was seen in the resulting voltammograms with increasing nitrogen flow rate. The measurements and experiments were carried out at ambient temperature, namely 23 ºC.

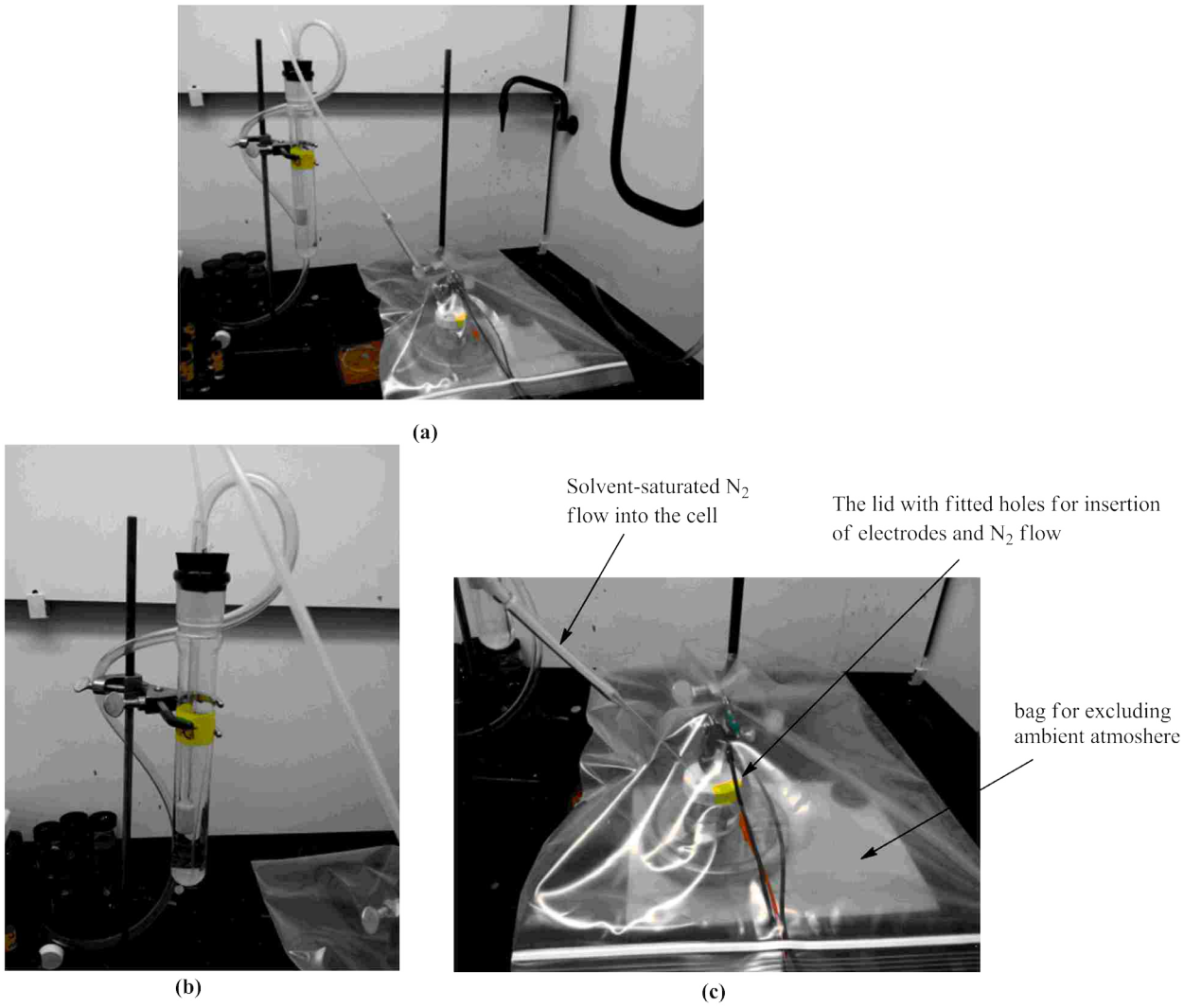

Figure 4.1 The apparatus of cyclic voltammetry described in this chapter: (a) overall view, (b) the setup for generating solvent-saturated N_2, (c) the three-electrode cell with a N_2 blanket.

For the CV tests done in aqueous solutions, the electrolyte used was 0.1 M KCl, and the CV tests done in DMSO were run with 0.1 M $TBAPF_6$ (tetrabutylammonium hexafluorophosphate) as the electrolyte. DMSO was used as a solvent in addition to water, because DMSO is electrochemically stable at the potentials used in the tests and also because it can likewise solvate the viologen species. The CV tests of MAV and APV were carried out in DMSO with concentration of approximately 1 mM. The CV tests of AAPB monomer were performed in a pH 12 aqueous solution and in DMSO. The concentration of AAPB monomer was approximately 10 mM in both solvents.

4.3 Results and Discussion

Voltammograms were used to obtain half-wave potentials ($E_{1/2}$), diffusion coefficients (D) and heterogeneous electron-transfer rate constants (k_{et}).

MAV and APV: Figure 4.2 shows a series of cyclic voltammograms in DMSO with 0.1M $TBAPF_6$ obtained at 200 mV/s. For each voltage loop or voltammogram, the more positive peaks represent the reduction current, and the more negative peaks represent the oxidation current. The horizontal offset between the reduction and oxidation peaks represents the degree of irreversibility. The voltammograms were stacked as shown in Figure 4.2 with vertical offset to ensure comparison. The curves of monomethyl viologen (MMV) and ethyl viologen (EV) are included in Figure 4.2 to compare with MAV and APV. Two oxidation and reduction waves are clearly seen for MAV (a disubstituted viologen), and one oxidation and reduction wave is seen for APV (a monosubstituted viologen). The monosubstituted viologens (APV and MMV) are shown to have similar redox potentials, and it is also the case for disubstituted viologens (MAV

and EV). But it is notable that the current peaks for APV are flatter and smaller than that of MMV; the difference can be attributed to the amine group of the APV.

Figure 4.2 Cyclic voltammograms of MAV, APV, MMV and EV in DMSO containing 0.1 M TBAPF6 and vs AgCl [21].

As shown in Figure 4.2, $E_{1/2}$ values (half wave potential), and ΔE_p values (the difference in potential between the anodic and cathodic potential) can be obtained. The $E_{1/2}$ values were calculated as $E_{1/2} = (E_{pc} + E_{pa})/2$, where E_{pc} is the potential at the cathodic peak and E_{pa} is the potential at the anodic peak (determined from voltage local extrema). The $E_{1/2}$ for APV is -0.83 V, and for the two redox potentials of MAV are -0.36 V and -0.72 V respectively. The ΔE_p for APV is 0.133 V and for MAV is 0.09 V [21].

The bulk diffusion coefficient (D) is an important factor to consider for a DCFC in which homogenous viologens are used as the catalysts. Values for D can be found with CV tests by using the Randels-Sevcik equation [50, 58, 59]:

$$i_p = 0.4463nR(\alpha a v)^{1/2} A D^{1/2} c \tag{4.1}$$

where $a = nF/RT$, n is the number of electrons exchanged during an oxidation or reduction step, F is the Faraday constant, T is the absolute temperature, and R is the ideal gas constant. i_p is the peak current. The measurement of i_p was done using the built-in analysis tool in the Gamry potentiostat, where peak baselines were drawn and the values of i_p for the reduction and oxidation peak were measured from the their corresponding peak baseline. The resulting i_p value was the average of the magnitudes of the reduction and oxidation peak currents. A is the surface area of the working electrode, α is the charge-transfer coefficient (α = 0.5 in this case for reversible reactions), and v is the scan rate. c is the bulk concentration of the oxidized species, which is constant and equal to the concentration of added viologen. This is confirmed by the presence of a deep purple color corresponding to the oxidized state.

Except for the diffusion coefficient, all the other variables are known in Equation 4.1. To prevent an inaccurate value of D caused by any particular scan rate, a plot of the peak current (i_p) vs. the square root of the scan rate ($v^{1/2}$) was made (see Figure 4.3). Such a plot is called Randles-Sevcik plot and should give a straight line passing through the origin. The slope of this line is proportional $D^{1/2}$. The D values generated in this way were 7.8×10^{-7} cm^2/s for MAV by taking the average of the two redox peaks, and 1.0×10^{-6} cm^2/s for APV. These differ slightly

from the previously reported values of 0.80 cm^2/s and 0.81 cm^2/s respectively [21]. This is because the previous fits of i_p vs. $\nu^{1/2}$ to get D did not enforce a required zero intercept. These are reasonable estimates for D given that the estimates of D from the Wilke-Chang equation are 1.69×10^{-6} cm^2/s for MAV and 1.82×10^{-6} cm^2/s for APV [60]. Using the Wilke-Change equation, the structure of APV was estimated based on 2 benzene rings and 1 C_3H_8, and for MAV the structure was estimated with 1 APV and 1 CH_4 [60].

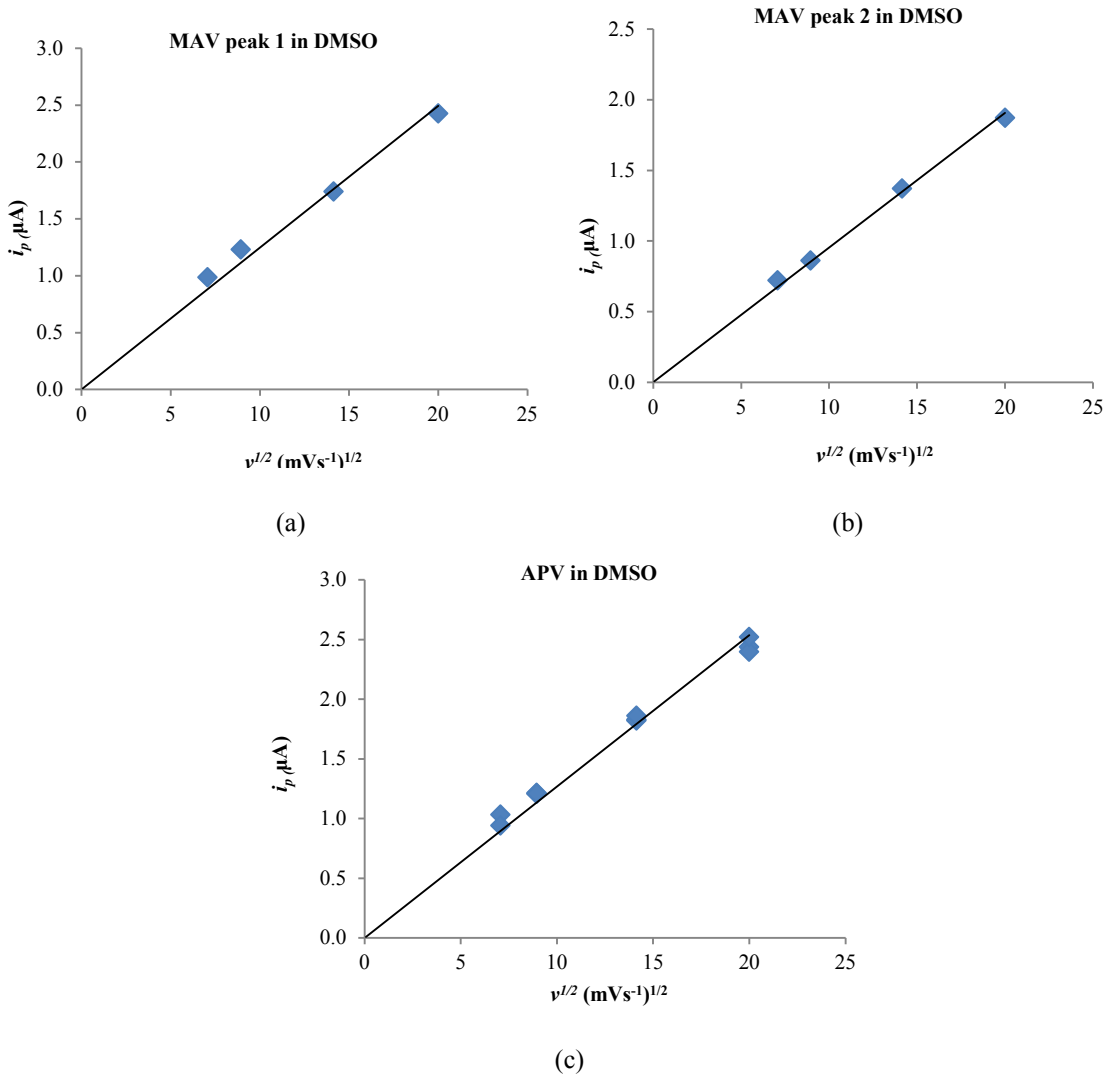

Figure 4.3 Calculation of D by plotting peak current (i_p) vs. square root of scan rate ($\nu^{1/2}$). Points are from experiments and lines are least square fit.

The ΔE_p information obtained from the CVs and the diffusion coefficients calculated above can be used to determine the heterogeneous electron-transfer rate constant (k_{et}). The k_{et} values are important to determine the usefulness of the tested viologen catalysts in their soluble forms in a fuel cell. The higher the value of k_{et}, the quicker the electrons can be transferred from viologen to the anode, and therefore the more efficiently the cell will oxidize the carbohydrate fuel and produce electricity. The k_{et} values were determined from an equation proposed by Nicholson [61]:

$$\Psi = \gamma^{\alpha} k_{\mathrm{et}} / (\pi a D_{\mathrm{O}} v)^{1/2} \qquad (4.2)$$

where $\gamma = (D_{\mathrm{O}}/D_{\mathrm{R}})^{1/2}$, and Ψ is a kinetic parameter and obtained from the Nicholson's paper, which is related to ΔE_p from the CV. D_{O} and D_{R} are the diffusion coefficients of the oxidized and the reduced species respectively, and are assumed to be approximately equal and to have the same value as D; so in this case, $\gamma = 1$. a is defined as the same as above. The final k_{et} values are the average of k_{et} calculated in the scan-rate range from 0.05 to 0.4 V/s. The calculated k_{et} for MAV is 2.9×10^{-3} cm/s, and for APV is 1.3×10^{-3} cm/s in DMSO solvent [21].

Table 4.1 shows a summary of D and k_{et} values of APV and MAV along with the other viologen molecules studied in Ref [21]. ACN is short for acetonitrile. All the viologens are monosubstituted except for ethylviologen (EV) and MAV, which are disubstituted.

Table 4.1 Diffusion Coefficients (D) and heterogeneous electron-transfer rate constant (k_{et}) of the tested viologens reported in Ref [21].

	D (10^{-6} cm^2s^{-1})		k_{et} (10^{-2} cm s^{-1})	
Species*	ACN	DMSO	ACN	DMSO
MMV	13.8	3.65	1.73	0.60
MEV	14.8		1.78	
MPV	18.0		2.03	
MBV	22.8		1.92	
EV	8.81	1.77	1.85	0.54
APV		1.00		0.13
MAV		0.78		0.29

*Abbreviations are as follows: MMV=monomethyl viologen, MEV=monoethyl viologen, MPV=monopropyl viologen, MBV=monobutyl viologen, EV=ethyl viologen, APV=aminopropyl viologen, MAV=methyl aminopropyl viologen

The D values, as expected, are larger in lower viscosity solvent ACN, as compared to higher viscosity DMSO. APV and MAV have smaller D values than do MMV and EV in DMSO. It is thought that the amine group on APV and MAV is likely the cause of the decrease in D. It has been shown that k_{et} is affected by temperature, solvent, and material of the working electrode [62]. The values of k_{et} obtained for MAV and APV are lower than those for the other tested viologen molecules in acetonitrile in Ref [21] under the same experimental condition, likely because DMSO is a more viscous solvent, making the electron-transfer process more difficult. However, the results of k_{et} values for MAV and APV are close to and in the same order magnitude as the value obtained for N-butyl viologen, namely 2.3×10^{-3} cm/s, in DMSO in Ref [62] using the same equation developed by Nicholson.

AAPB monomer: Figure 4.4 shows cyclic voltammograms of the AAPB monomer in (a) DMSO with 0.1 M $TBAPF_6$ and (b) in a pH 12 aqueous solution with 0.1 M KCl. A pH 12 solution was used to imitate conditions for the intended fuel cell operation.

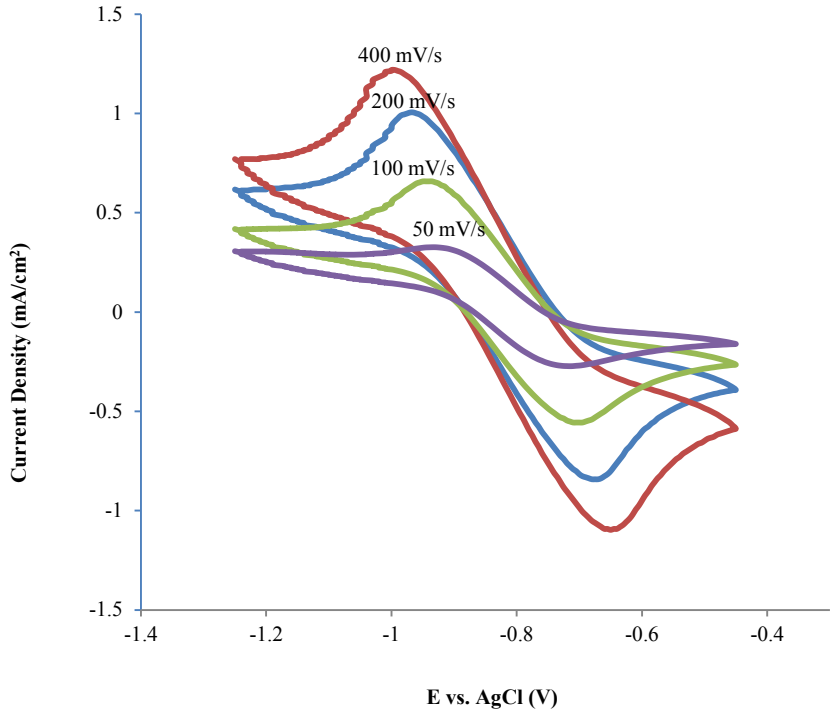

(a)

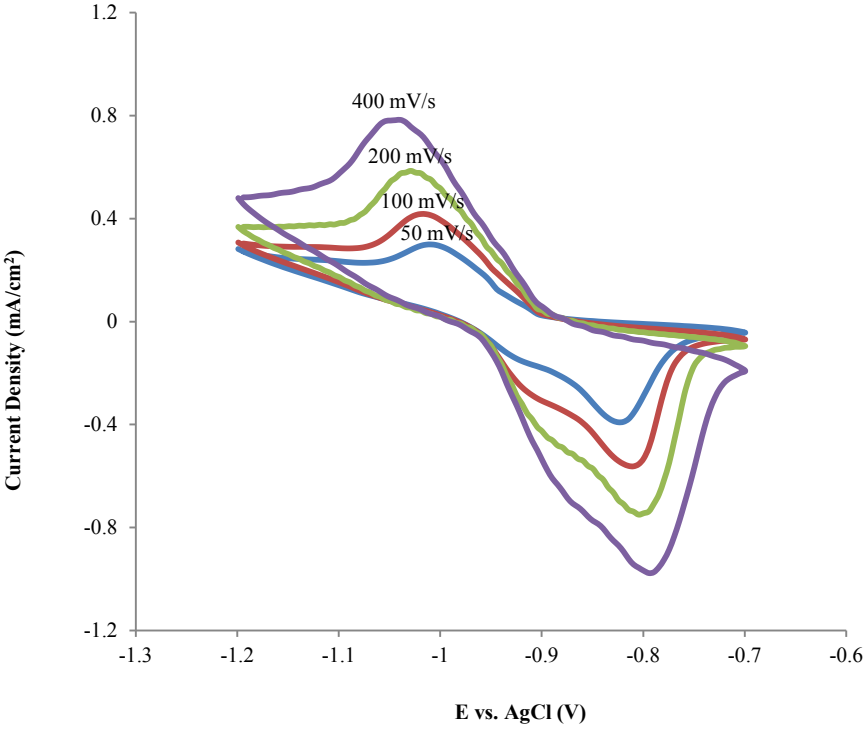

(b)

Figure 4.4 Cyclic voltammograms of AAPB monomer (a) in DMSO containing 0.1 M TBAPF6, (b) in pH 12 aqueous solution containing 0.1 M KCl.

For both cases, the CVs were recorded at different scan rates ranging from 50 to 400 mV/s. The potentials were scanned between -0.4 V to -1.2 V for the voltammograms carried out in DMSO, and between -0.7 V to -1.2 V for the basic solution. In the range of the potentials scanned, the AAPB monomer shows electroactivity in DMSO and basic aqueous solution as one oxidation and reduction wave are seen for each case. The observed oxidation-reduction process is reversible. As expected, the peak currents decrease at decreased scan rates.

As shown in Figure 4.4, the AAPB monomer behaves slightly differently in aqueous solution than it does in DMSO. The notable difference is that the oxidation peak has a greater magnitude than the reduction peak in the aqueous solution (approximately 1 mA/cm^2 for oxidation peak and 0.8 mA/cm^2 for reduction peak), whereas the magnitudes of the oxidation and reduction peaks are equal in DMSO (approximately 1.2 mA/cm^2 for both oxidation and reduction peaks). Also, the AAPB monomer has a small bump half way up the oxidation peak in the aqueous solution, while it has clean and sharp peaks in DMSO. The above-mentioned differences may be due to the fact that some of AAPB monomers in the aqueous solution were absorbed on and oxidized by the working electrode. When they are absorbed on the working electrode surface, they may act as their analogous disubstituted type, which may likely cause the small bump.

$E_{1/2}$ for the monomer in DMSO is -0.82V, and ΔE_p is 0.275V. $E_{1/2}$ of the monomer in DMSO is very close to that for the APV. In aqueous solution, $E_{1/2}$ and ΔE_p are -0.92V and 0.211V respectively. Figure 4.5 locates the redox potential of the AAPB monomer on the Poubaix diagram (see Figure 2.5) along with that for methyl viologen (MV) and monomethyl viologen (MMV). The redox potential of the monomer is more negative than that of MV, and is close to but slightly more positive than that of MMV. This means that the monomer has a similar

open circuit potential as MMV does, and has a higher energy output than that for MV but may react slower because of less thermodynamic driving force for catalytically oxidizing carbohydrates.

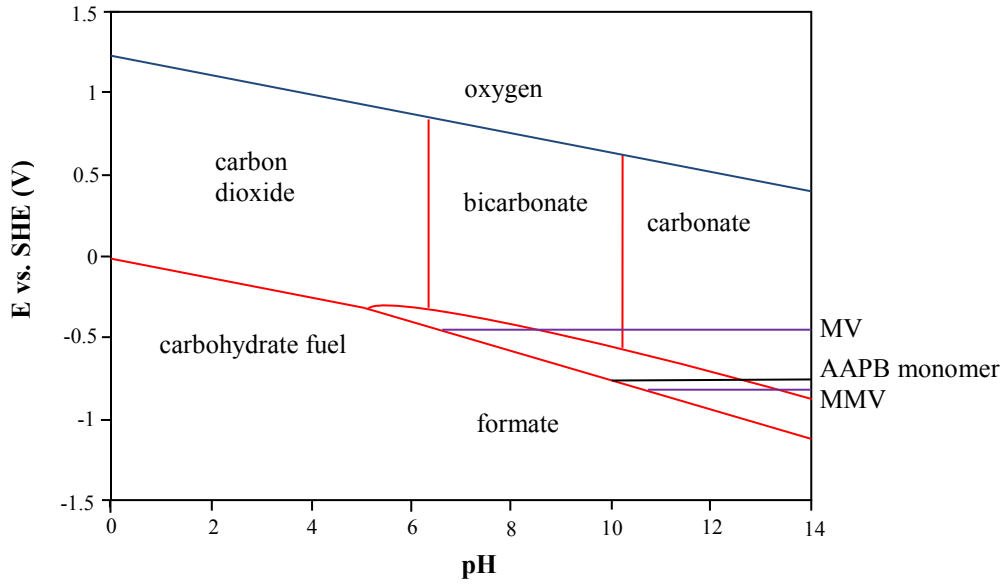

Figure 4.5 Pourbaix diagram for carbohydrate redox system, modified from Ref [21]. Included here are the redox potentials of methyl viologen (MV), monomethyl viologen (MMV) and the AAPB monomer.

The values for D of the monomer in DMSO and in aqueous solution were calculated, based on the method discussed above (Equation 4.1). Figure 4.6 shows plots of the peak current (i_p) vs. the square root of the scan rate ($v^{1/2}$) of the monomer in DMSO and in aqueous solution respectively. The D value of the monomer generated from the slope in DMSO is 0.99×10^{-6} cm^2/s, and in aqueous solution is 3.13×10^{-5} cm^2/s.

The k_{et} values were then determined according to Equation 4.2 using the obtained D values and the kinetic parameter, ψ. The value of ψ can be obtained from a table in the Nicholson paper and is related to ΔE_p from the cyclic voltammograms. Because the ΔE_p values in DMSO and in aqueous solution for the monomer are out of the range of ΔE_p values listed in the

Nicholson table, the values of ψ used here were extrapolated from a trend line of the Nicholson data. This procedure is shown in Appendix A. The k_{et} value of the monomer in DMSO is $1.0\times1v0^{-4}$ cm/s, and is 1.5×10^{-3} cm/s in aqueous solution.

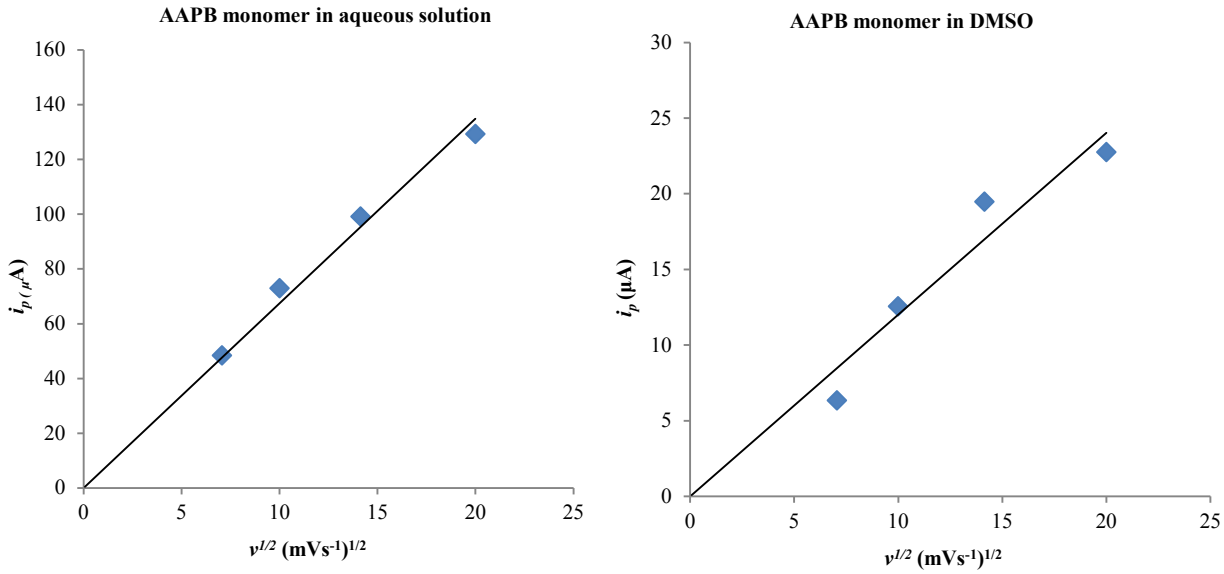

Figure 4.6 Calculation of *D* by plotting peak current (i_p) vs. square root of scan rate ($v^{1/2}$) for AAPB monomer in (a) aqueous solution and (b) in DMSO.

Table 4.2 summaries the values of D, k_{et} and ΔE_p of the monomer, as well as those of APV and MV, included for comparison. Among other viologen molecules investigated here and in Ref [21], the APV structure is most similar to that of the monomer. Basically the monomer is APV with an amide group connected to the amine. MV is the only viologen molecule whose D and k_{et} values were reported in aqueous solution, in this case at pH 7 [21]. Even though MV has rather different molecular structure than the monomer does, it is still helpful to have some sort of baseline to compare the electrochemical properties of the monomer in aqueous solution.

Table 4.2 Diffusion coefficient (D), heterogeneous electron-transfer rate constant (k_{et}) and ΔE_p values in DMSO and H_2O.

	D (10^{-6} cm^2s^{-1})		k_{et} (10^{-2} cm s^{-1})		ΔE_p (mV)	
Species	DMSO	H_2O	DMSO	H_2O	DMSO	H_2O
AAPB	0.99	3.13	0.02	0.23	275	211
APV	1.00		0.13		133	
MV		8.40		1.70		80

In comparison with the measured D value for APV in DMSO, the monomer has a slightly smaller value. It is probably due to the extra amide group that makes a more bulky structure, making it more difficult to diffuse in DMSO. The monomer has a 2-order-of-magnitude lower k_{et} value compared with that of APV. In aqueous solution, the D value of the monomer is the same order of magnitude as for MV and somewhat smaller. However, for the intention of immobilization of the monomer, the impact of the diffusion coefficient on the catalytic efficiency may become less significant. Instead, the k_{et} value is a more important factor to consider, particularly in aqueous solution. The k_{et} value of MV is almost 8-fold greater than the value obtained for the monomer, meaning that the electron-transfer rate is relatively slow for the monomer. This may be attributed to the fact that the oxygen in the amide group and the nitrogen in the amine group can form hydrogen bonding with water molecules or hydrogen bonding between monomers. The hydrogen bonding restricts rotation and movement and therefore could interfere with the electron transfer process of the monomer, which therefore can potentially restrain the rate of catalytic oxidation of carbohydrates.

4.4 Conclusion

An electrochemical investigation by cyclic voltammetry (CV) of methylaminopropyl viologen (MAV), aminopropyl viologen (APV) and the novel viologen (AAPB) monomer are

presented. Our results demonstrate that the AAPB monomer is electroactive under the basic conditions that are desirable for our fuel cell operation, and shows similar $E_{1/2}$ redox potential to other studied monoalkyl viologens. The electroactivity of the AAPB monomer in its homogenous form indicates that the monomer can potentially catalyze carbohydrates fuel as efficiently as other monosubstituted viologens do. The diffusion coefficients (D), heterogeneous electron-transfer rate constants (k_{et}) were reported for MAV and APV based on joint work reported in Ref [21]. Following the same methods, the D and k_{et} values were calculated for the AAPB monomer in this chapter. It was found that the monomer in its soluble form has similar or even greater diffusivity compared to other viologen molecules in DMSO and aqueous solutions, but has much lower k_{et} values, which may potentially be a drawback of its being used as a catalyst in our DCFC system.

5 Electrodeposition of the Viologen Monomers and Electrochemical Investigation of Their Immobilized Viologen Polymer for Use in a Direct Carbohydrate Fuel Cell

5.1 Introduction

Viologen must be immobilized on a surface in practical direct carbohydrate fuel cell (DCFC) devices because of cost and the oral toxicity of viologen. Prior results discussed in Chapter 2 also showed that there is also an advantage of utilizing polymeric viologens to increase the local concentration of catalyst in order to prevent formation of unreactive intermediate product during the glucose oxidation, and therefore to increase the fuel cell efficiency.

Our immobilization effort involved attaching the novel viologen monomer (AAPB) reported in Chapter 3 to an electrode surface. The attachment was carried out by electroreductive polymerization of the viologen monomer. In other words, the polymerization was initiated by electrons and as a result, a polymeric viologen coating was formed on the electrode surface. The idea of immobilization of the viologen monomers by electropolymerization is adapted from the work carried out by Katz et al. [48], where they electrolyzed sodium acrylate in the presence of Zn^{2+} to yield a polymeric coating on a gold electrode. The formation of the acrylate polymer was reported to start and propagate at the terminal acrylate group. This method was chosen because our viologen monomer has an acrylamide group at the end of the molecule. The structure of

acrylamide is similarly to that of acrylate, basically replacing –OH with $–NH_2$. And acrylamide was also reported for electroinitiated polymerization in the presence of Zn^{2+} [63, 64].

Gold surfaces and graphite surfaces were used as substrate for the attachment. Gold was chosen because it is stable and unreactive with a wide range of electrolytes. Moreover, a gold surface was used here for the purpose of imitating Katz's experiment as an initial examination of the electropolymerization technique. The reason for using graphite is that carbon (usually in the form of carbon black) is widely used as an anode catalyst substrate in commercial fuel cells. In this work, a graphite disk was used for prototype or testing purposes.

The electroactivity of the viologen-modified electrode was investigated toward oxidizing carbohydrates under desired DCFC operation conditions, using a viologen-coated graphite disk. The immobilized viologen coating was found to have low catalytic activity toward oxidizing carbohydrates. Therefore, we performed additional tests to discover the cause of the low electroactivity. We found that the soluble viologen monomer and viologen polymer in solution are electroactive toward oxidizing carbohydrates, and the viologen-polymer coating on a graphite disk is not an insulation layer that blocks electron transfer.

5.2 Experimental

5.2.1 Methods

The examination of the eletrodeposition of the polymeric viologen film was performed with different tools, including scanning electron microscopy (SEM), energy dispersive X-ray spectroscopy (EDAX), X-ray photoelectron spectroscopy (XPS), and measurement of water contact angle.

5.2.2 Materials

The following materials were used for electropolymerization experiments and fuel cell tests. Zinc chloride and N,N'-methylenebisacrylamide were purchased from Fluka Chemicals. Ammonium chloride was obtained from C.C.I. Chemicals. Sodium citrate was purchased from EM Science. Gold potassium cyanide was purchased from GFS Chemicals. Nickel wire (0.5mm diameter) and sodium hypophosphate were supplied from Fisher Scientific. Graphite disks (0.5cm diameter) were custom-machined by Mersen USA Greenville, Corp. 2000-grit sandpaper was obtained from 3M, and qualitative-grade filter paper was supplied from VWR Chemicals. The novel viologen monomer (AAPB) was synthesized in-house as discussed in Chapter 3. Potassium hydroxide, dihydroxy acetone (DHA), fructose and potassium phosphate were obtained from Sigma-Aldrich. All chemicals were used with no purification. The water used for solution was double-distilled.

5.2.3 Preparation of Electrodes

Gold plating on nickel wire: A gold surface was prepared by an electroless plating technique on nickel wire with diameter 0.5 mm. The plating bath was prepared with 0.02 g gold potassium cyanide, 0.75 g ammonium chloride, 0.57 g sodium citrate, and 0.1 g sodium hypophosphite, all added to 15 mL of double-distilled water. The measured pH was 7-7.5. The plating bath was firstly heated to boiling and then the temperature was reduced to around 50-60 ºC. The nickel wire was then added to the bath. After 1 hour of plating the wire was fully covered with a gold layer of 400 nm average thickness as determined by SEM, and was rinsed with double-distilled water.

After 1 hour of plating the wire was fully covered with a gold layer of 400 nm average thickness and a similar level of roughness, and was rinsed with double-distilled water

Graphite disk: Prior to the electropolymerization step a graphite disk was polished on the end with a piece of 2000-grit sandpaper, and then wiped with Kimwipe. The surface was further polished on a piece of qualitative-grade filter paper. The resulting surface was flat and shining. The polished graphite disk was not rinsed or washed, and directly used for the next step of the experiment.

5.2.4 Electropolymerization

A 10 mL aqueous solution containing 3.48×10^{-2} g (approximately 0.1 M) AAPB monomer, 1.36×10^{-3} g (0.1 mM) $ZnCl_2$ and 6.8×10^{-2} g (0.4 mM) N,N'-methylenebisacrylamide, was used to produce a polymeric layer on the gold or carbon surface. The prepared electropolymerization solution was stored in a refrigerator before use. The electropolymerization was carried out at a potential of -1.297 V vs Ag/AgCl for 15 minutes. The electrochemical reduction of the monomers also introduced the reduction of Zn^{2+} with an accumulation of Zn crystals on the electrode surface. To strip the Zn, -0.673 V vs. Ag/AgCl was imposed on the electrode surface for 10 seconds. After the electropolymerization and stripping the electrode was rinsed several times with double-distilled water. Attempts to carry out the electropolymerization at other different potentials and different plating times were also done.

5.2.5 Fuel Cell

For soluble viologen monomer: The apparatus for the fuel cell test of the homogeneous viologen monomer was carried out using the same setup as described in Section 2.7 (See Figure 2.11). The electrolyte used was 1 M KOH. The 1 M KOH solution was purged with nitrogen for

10 minutes before being added to the anode compartment. At the same time, nitrogen was blown into the closed bag to create a low oxygen environment. After the anode compartment was filled with the deoxygenated 1 M KOH, a reference electrode was placed and all electrical connections were then put in position. Once the cell was on and current was stabilized, fructose was added to the cell. Lastly, AAPB monomer was added with a glass syringe. The experiment was performed at a constant potential with a Gamry PC4/750 Potentiostat.

For viologen-covered graphite disk: Fuel cell tests for viologen-covered graphite disks were conducted with a cell device that is a modification of the apparatus shown in Figure 2.11. Figure 5.1 shows the modified fuel cell arrangement. The functions of the stir bar and the nickel foam were replaced with a rotating graphite disk electrode fitted in a Teflon holder. A fitted hole on the top of the anode compartment was made for insertion of the rotating disk electrode to contact the anode solution. The experiments were carried out using an Arbin BT2000 Potentiostat, and the data was set to be collected every 0.1 second to achieve a smooth curve by minimizing the background noise. The rotation speed of the rotating electrode was set at 200 rpm for all tests.

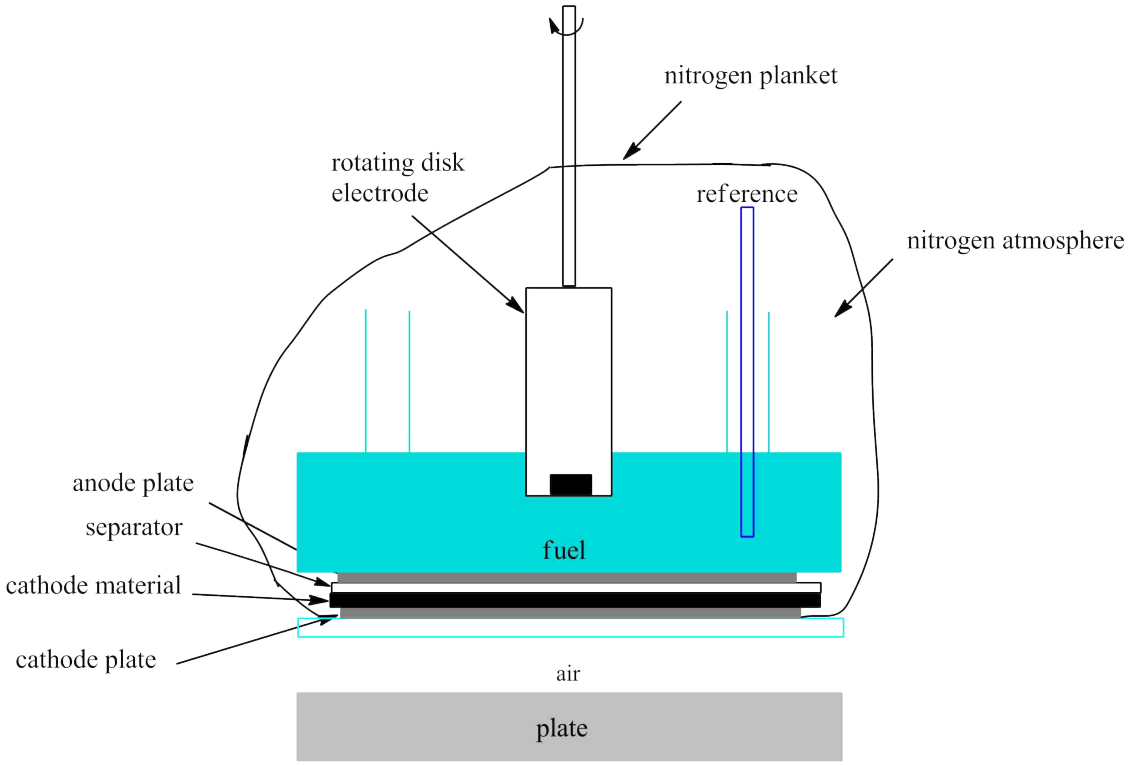

Figure 5.1 Modified fuel cell-like device for viologen-modified carbon disk electrode.

The electrolyte was a 0.2 M phosphate pH 12 buffer solution. Following the same procedure as discussed above, oxygen was excluded from the electrolyte by purging nitrogen for 10 minutes before the electrolyte was added to the anode compartment. Simultaneously, the nitrogen atmosphere was maintained in the closed bag. The test was conducted at 0 V; once the current reached plateau, DHA was added to the anode compartment.

For both cases stated above, to ensure repeatability, the air cathode material was soaked in 6 M KOH for at least 24 hours before being used in the cell. The air cathode was then rinsed with double-distilled water and patted dry before the cell was assembled.

5.3 Results and Discussion

5.3.1 Electropolymerization

Previous reports showed that the electropolymerization of acrylamide in the presence of Zn salts involves formation of a complex of Zn^{2+} with acryl derivatives [63, 65]. As an acryl derivative, the AAPB monomer should have similar reaction mechanics to that observed with acrylamides. Equations 5.1 to 5.5 show the proposed electropolymerization reaction pathway of AAPB monomers in the presence of Zn^{2+}. ACM represents acrylamide monomer. The following mechanism supports the probable intervention of a monomer-zinc-cation complex as the responsible initiator species. The partial donation of carbonyl electrons to the zinc cation species, shown as $ZnOH^+$, can be expected to produce partial delocalization of electrons of the carbon-carbon double bond, and therefore the bond is electron-deficient and more readily accepts cathodic electron than does uncomplexed monomer. It was proposed that acrylamide monomer is complexed with $ZnOH^+$ in a six-member ring [63]. In this case the proposed six-member ring structure for our viologen is illustrated in Figure 5.2. A direct reduction of Zn^{2+} also takes place, with accumulation of Zn crystals on the surface of the polymer. To solubilize the deposited Zn, oxidation of the electrode at a positive potential was carried out.

$$Zn^{2+} + H_2O \rightleftharpoons ZnOH^+ + H^+ \quad (5.1)$$

$$ZnOH^+ + ACM \rightleftharpoons ZnOH^+\text{-}ACM \quad (5.2)$$

$$ZnOH^+\text{-}ACM + e^- \longrightarrow ZnOH^+\text{-}ACM^- \quad (5.3)$$

$$ZnOH^+\text{-}ACM^- + H^+ \longrightarrow ZnOH^+\text{-}ACMH\cdot \quad (5.4)$$

$$ZnOH^+\text{-}ACMH\cdot + m\text{ACM} \longrightarrow \text{polymerization} \quad (5.5)$$

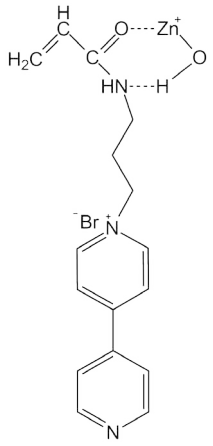

Figure 5.2 Six-member ring structure of Zn complex associated with viologen monomer.

Gold surface: Examinations by scanning electron microscopy (SEM) of the gold electrode before and after the electrochemical treatments are shown in Figures 5.3 and 5.4. Figure 5.3 shows an image of a virgin gold surface before electropolymerization, showing some variability in roughness. Figure 5.4 represents different views of the gold surface after electropolymerization of the AAPB monomers and demonstrates the formation of polymer film on a gold surface. The morphology of the viologen polymer coating is consistent with that of other polyacrylamide coatings on the gold surface presented in the previous studies [48, 66]. The polymer coating appeared to be uniformly web structured.

The coated gold electrode was also examined by EDAX, which was used for identification of the elements. Figure 5.5 shows the EDAX spectrum of the viologen-polymer-covered gold surface. A 5 kV electron beam was used, which is typical for surface chemical characterization. EDAX analysis shows that N, O, and C elements were detected on the surface. This further proves the formation of viologen polymer. On the other hand, there was some Zn also detected. It has been reported that 5 s of the oxidative treatment at -0.673 V vs. Ag/AgCl

should be sufficient to solubilize the Zn crystals accumulated during the electropolymerization process. The presence of Zn was examined by the energy-dispersive X-ray analysis, and showed showing no Zn residual detected [48]. But, 10 s of the oxidative treatment in this work still resulted in unremoved Zn as discussed below. At present we have not found a satisfactory explanation for the origin of these discrepancies.

The surface element content included in Figure 5.5 gives a qualitative estimate, and should not be considered quantitative. For EDAX quantitative analysis there are some very specific requirements in order for the results to be reliable [67]: (1) the sample must be polished flat to at least 0.5 micron sized grit; (2) the sample must be homogeneous in the volume being excited; and (3) the sample must be stable under the electron beam. Our viologen-polymer-coated gold sample meets the last requirement, but not the first two. As mentioned before, the plated gold layer is around 400 nm. The coated-polymer layer is estimated between 30-100 nm thick. Additionally, the surface of our sample has roughness with size scale around 1 μm. Therefore, the composition results given by EDAX for our sample are not completely reliable. At this point, a significant amount of Zn was detected but it is unknown exactly how much was present. The significant observation is the presence of N, which comes from the viologen and the amide group in the polymer.

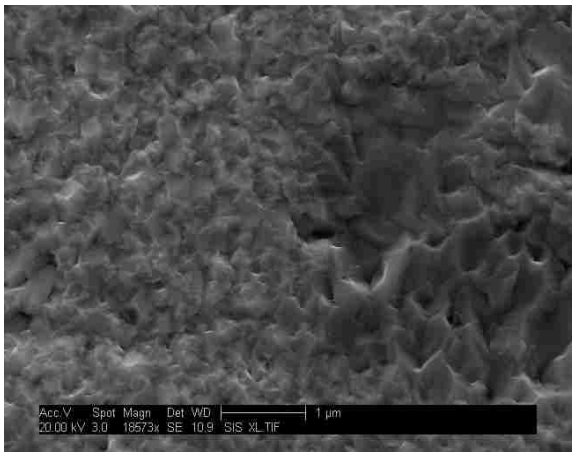

Figure 5.3 SEM image of a bare gold surface (surface of gold plated nickel wire) .

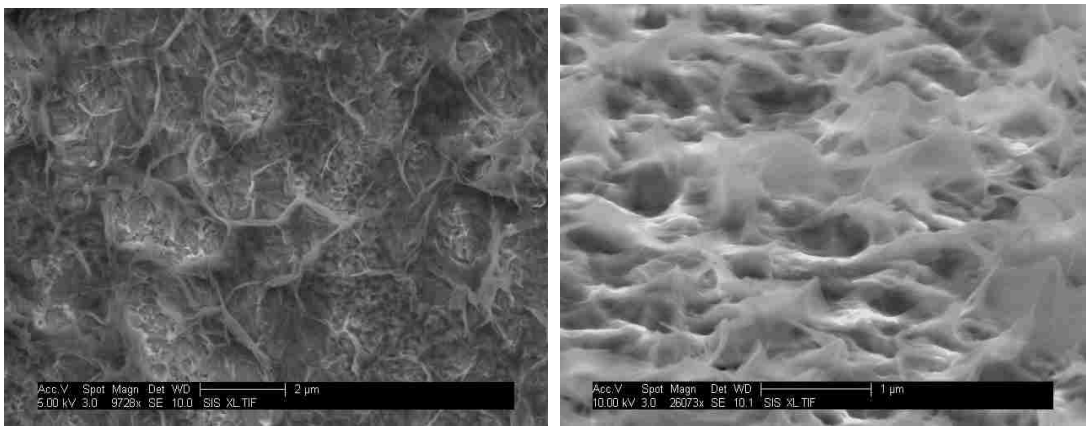

(a) (b)

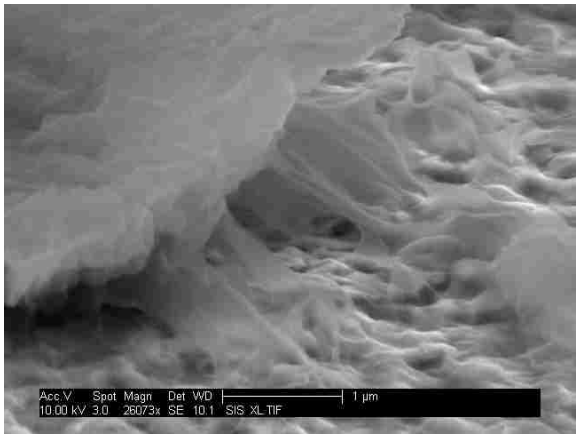

(c)

Figure 5.4 SEM images of viologen polymer coating on gold surfaces. a) top view, b) side view and c) a close view of polymer coating.

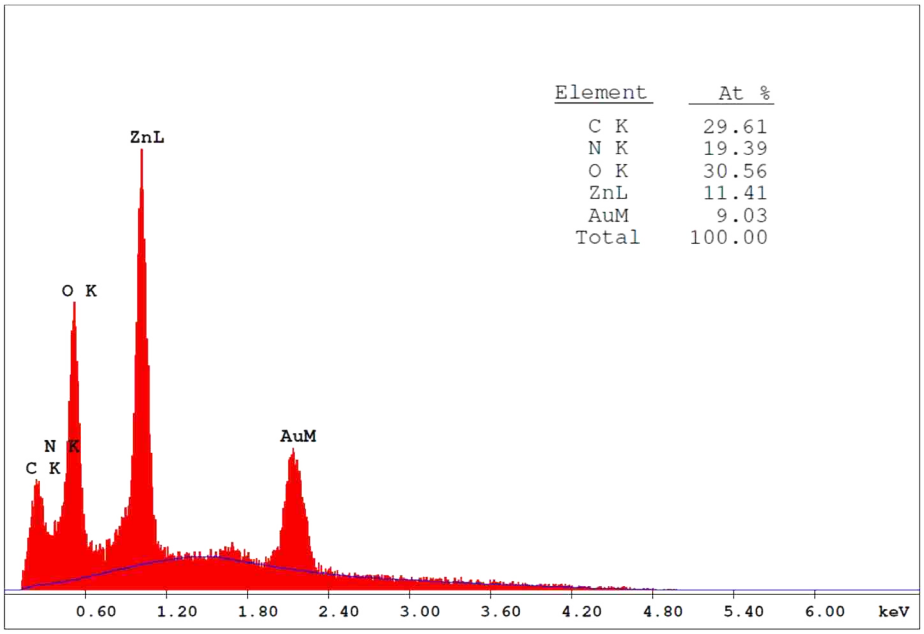

Figure 5.5 EDAX analysis of viologen-polymer-coated gold surface.

Graphite surface: As mention earlier, the electropolymerization of viologen monomers on graphite surface followed the same procedure for that on gold surface. To our knowledge, there has been no previous report on directly electropolymerizing acrylamide monomers or viologen monomers on a graphite surface. Examination of the polymer formation on graphite surface by SEM is shown in Figures 5.6 and 5.7. Figure 5.6 shows an image of polished bare graphite surface before the electrochemical treatments, and Figure 5.7 shows an image of graphite surface afterwards with formation of polymer coating. The structure of polymer coating on graphite surface is similar to that on the gold surface. To further verify that the Zn complex can induce the polymerization on a graphite surface, $ZnCl_2$ was replaced with KCl during the electropolymerization step. It was found that there was no polymer coating on the graphite surface following the intended polymerization steps as shown in Figure 5.8, indicating that the induction effect of Zn complex on polymerization also works on a graphite surface.

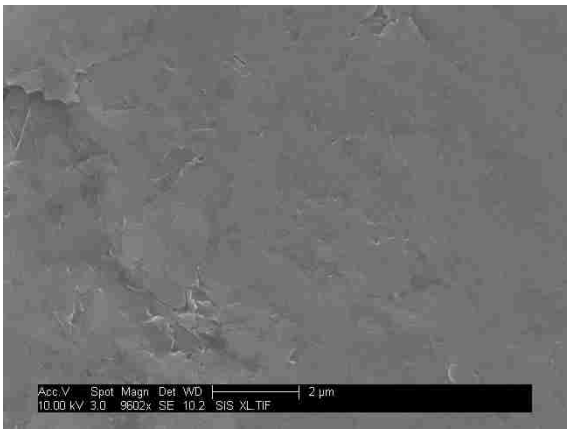

Figure 5.6 SEM image of polished blank graphite disk surface.

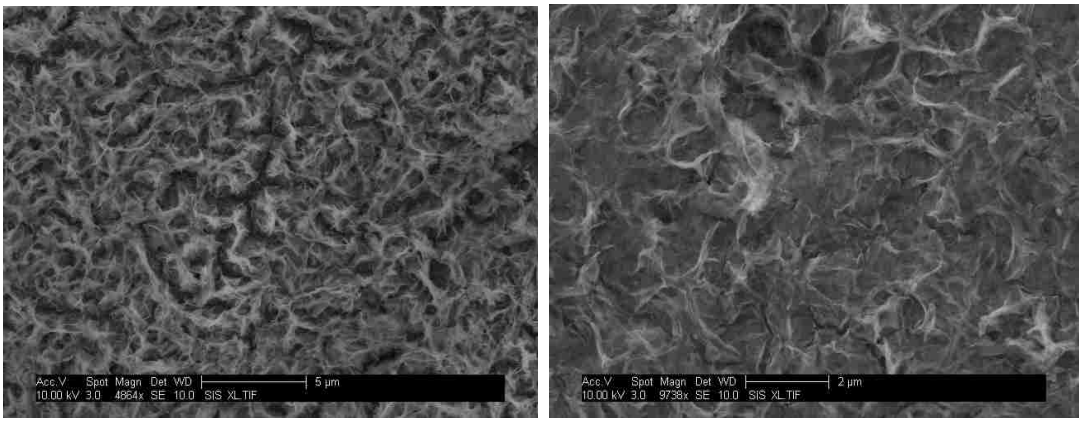

(a) (b)

Figure 5.7 SEM images of viologen polymer coating on graphite surface. (a) A broad view, (b) a close view.

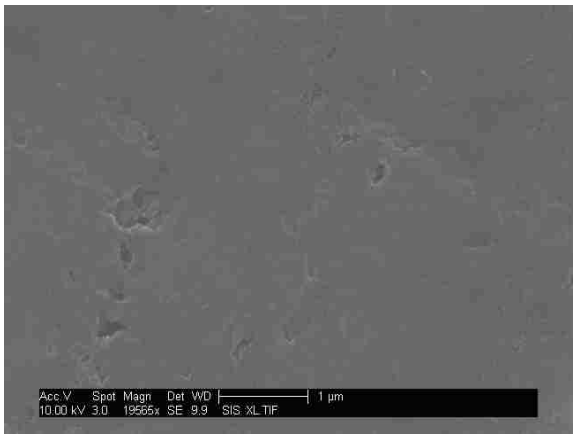

Figure 5.8 Graphite disk surface after electropolymerization in the presence of KCl instead of $ZnCl_2$.

Viologen-polymer-coated graphite disk were examined with respect to water contact angle, using a goniometer (Rame-Hart, Inc., Model 100-00 115)). There were three disk samples prepared for the measurement. Sample 1 was a blank-polished graphite disk; sample 2 was treated with electropolymerization for 1 minute; and sample 3 was treated with electropolymerization for 15 minutes. The first two samples were used for the purpose of control and comparison. Each water contact angle was the average of three determinations. The contact angels are 91°, 58°, and 51° for sample 1, 2 and 3, respectively.

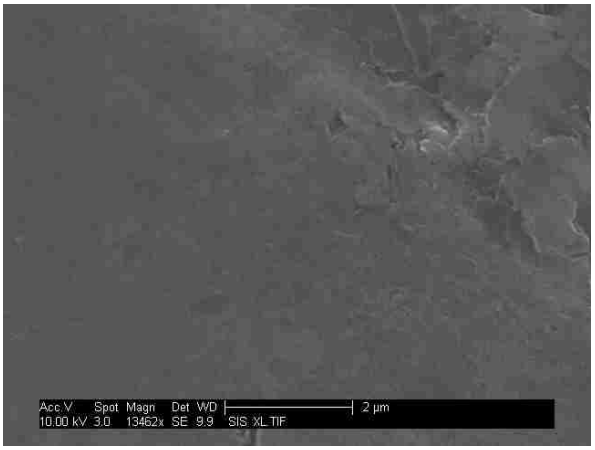

Figure 5.9 Graphite surface after 1-minute electropolymerization treatment.

Water contact angle measurement is to test the wettability of a solid surface. The higher the contact angle is, the more hydrophobic the surface is. It was found that the contact angle of the blank graphite disk is 91°, as expected for non-polar and therefore hydrophobic graphite. After being electro-treated with the viologen monomer in solution, the graphite surface became more hydrophilic as the viologen-polymer coating is polar. The contact angles after electropolymerization are much lower than that of blank graphite disk. The contact angle tends to decrease as the electropolymerization time increases. The lower value for 15-minute treatment is

due to greater polymer coverage and thick coating that can be seen under SEM as shown in Figure 5.7. In contrast, the 1-minute treatment does not produce a coating substantial enough to be observed by SEM as shown in Figure 5.9.

XPS was also used to verify the viologen-coating on the graphite disks. Table 5.1 shows the XPS surface atomic ratios of viologen-coated graphite disks. The XPS was quantitative analysis for C, O and N, and qualitative analysis for Zn. The graphite disks were the same samples prepared for water contact angle measurement as described above. The blank surface had no N element identified. On the other hand, N was detected on the samples treated with the 1-minute and 15-minute electropolymerization processes. For the 15-minute treatment, the ratio between N and C is 0.06, which is much lower than the theoretical value, 0.2, for the viologen polymer. This ratio is 0.02 for 1-minute treatment, which is expected because of the shorter electropolymerization time. In addition, there was some Zn detected for the sample having the 15-minute treatment, but not for 1-minute. To completely eliminate the apparent Zn on the surface, we tried to increase the anodic stripping potential to a more positive value, namely 0.039 V vs. Ag/AgCl; and we attempted to carry this stripping process from a period of 10 seconds to 5 minutes, nevertheless residual Zn continued to be detected. We presume that some Zn is strongly bound to the polymer coating.

As discussed earlier there was no SEM-observed coating on the 1-minute graphite surface, even though N atoms are present detected by XPS and the contact angle is lower than that of the blank graphite surface. There are a couple of possible explanations: (1) there was a viologen coating formed on the surface during the 1-minute electropolymerization process, but it is too thin to be seen under SEM; (2) the detected N element and increase of O content is due to some unwashed viologen monomers that were stuck on the surface, or the monomer may have

been absorbed on the surface by associating with some functional groups on the graphite surface. From the result of 15-minute treatment, we believe the first option is more likely. Option 2 is rejected because the XPS ratio is not consistent with the expected composition of monomer shown in table. From the results of 1- and 15-minute treatments, the surface composition is not what we expected for a polymer coating; it is possible that some contamination occurred before the XPS or during storage.

Table 5.1 Surface XPS atomic percentages and ratios of viologen-coated graphite disks.

Element	Blank	1 min	15 min	Expected ratio for monomer	Expected ratio for polymer
C	91.32	81.69	44.13	78.95	78.95
O	8.68	16.36	53.15	5.26	5.26
N	0.00	1.95	2.72	15.79	15.79
Zn	absent	absent	present	–	–
N/C	0.00	0.02	0.06	0.20	0.20
O/C	0.10	0.20	1.20	0.06	0.06

Effect of surface roughness: During the course of electropolymerization experiments of AAPB monomers, we also used a piece of gold sheet (Sigma Aldrich) as the substrate for the polymer coating. The surface of this gold sheet is flat and smooth on 1 μm length scale, as shown in Figure 5.10 (a). The electropolymerization experiment followed the same procedure as for those performed on the gold-plated nickel wire and graphite disk for 15 minute. We found that on the smooth gold sheet there was no polymer coating seen under SEM, except of some Zn deposition as shown in Figure 5.8 (b). The Zn crystals or clusters that were formed were verified by EDAX. There are two possible hypotheses to explain the absence of the polymer film following the electropolymerization steps on the gold sheet surface: (1) there was no viologen

polymer formed in the first place, or (2) there was viologen polymer formed but it did not remain on the surface. It is unlikely that the gold sheet electrode cannot initiate the polymerization since it is made of the same material used in the experiments mentioned above. On the other hand, if the latter hypothesis is true, this indicates that the polymer coating has a greater tendency to stay on a rough or defective surface, such as the gold-plated nickel wire or graphite disk. This may be attributed to the fact that the roughness and surface defects can provide sufficient mechanical interlocks that anchor the polymer and physically hold it onto the surface. The polymer itself is expected to be water soluble, so it may easily wash off.

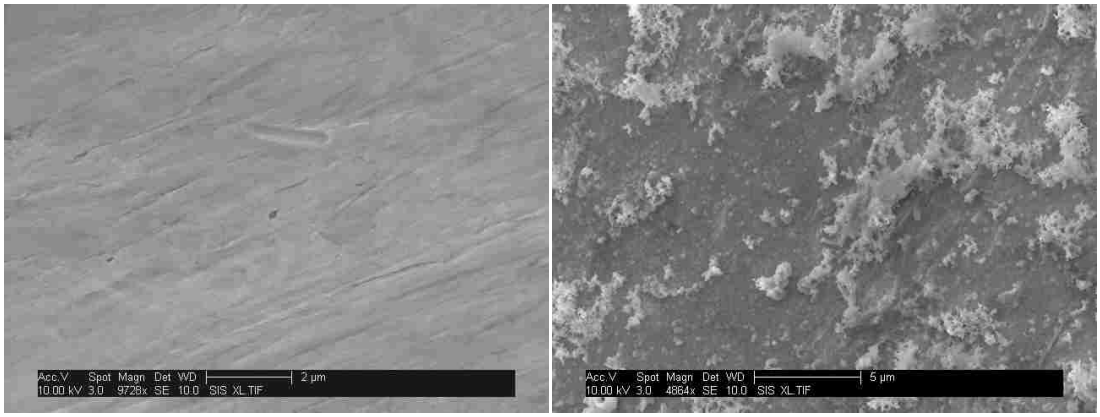

(a) (b)

Figure 5.10 (a) SEM image of an untreated gold sheet. (b) Zn crystals subsequently formed on the gold sheet.

5.3.2 Fuel Cell Test of Immobilized Viologen Polymer

The performance of the immobilized viologen polymer on graphite electrodes with respect to its catalytic ability to oxidize carbohydrates was determined by fuel cell tests using the in-house modified-fuel-cell apparatus described in Figure 5.1.

As aforementioned, the optimum operating condition of our DCFC is between pH 11-14, therefore the fuel cell tests for the immobilized viologen polymer were carried out in a 0.2 M phosphate buffer solution at pH 12. The buffer solution was purged with nitrogen for 10 minutes prior to being added to the cell; meanwhile, nitrogen was blown into the fuel cell closure bag to exclude oxygen. Any oxygen in the cell affects the extent of viologen catalytic reaction on carbohydrates because oxygen readily oxidizes MV^{1+} to MV^{2+} or MV^{0} to MV^{1+}, depending on what type of viologen is present. Also, in the presence of hydroxide, oxygen directly oxidizes carbohydrates and makes them inactive towards the viologen [68].

A 6 mL of the quasi-anaerobic pH 12 buffer solution was first added to the cell, then a rotating electrode with the viologen-modified graphite disk was inserted into the anode compartment through a hole, making contact with the electrolyte solution. No gas bubbles were observed on the surface of the graphite disk. The reference electrode was then placed in the cell. The cell was then set at 0 V vs. Ag/AgCl and recording for the test began. Once the current stopped fluctuating, 10 μL of 0.5 M DHA was added.

DHA, a carbohydrate-like molecule, was used as the fuel in these experiments. DHA was chosen because it is a relatively small molecule compared to other carbohydrates, like fructose or glucose, so it is expected to diffuse and interact with the immobilized viologen faster. It is also a very promising fuel source of a future commercial fuel cell, as it can be readily derived from glycerol (DHA and glyceraldehyde), which is a byproduct of biodiesel production. A potential of 0 V vs. Ag/AgCl was chosen because according to the Pourbaix diagram (see Figure 4.5), the chosen potential (0.205 vs. SHE) is more positive than the redox potential of AAPB monomer. After the viologen monomer oxidizes the DHA fuel, the more positive electrode can oxidize the

reduced viologen monomer. Therefore, we would expect to see a current increase after carbohydrate (DHA) is added to the cell.

For the viologen-polymer-coated graphite disk, the current showed an increase of 2 μA upon the addition of DHA. Such a low level of current generation does not demonstrates sufficient electro-catalytic ability of viologen monomer oxidizing carbohydrate. It is within the background noise from the instrument, which is ±3 μA according to manufacturer specification. To further prove the electroactivity of the immobilized viologen polymer toward the carbohydrates oxidation, we also tried films obtained at other electropolymerization conditions, such as at different potentials and for different time periods. The other attempts included 2 V, 0.5 V and -0.673 V, and at each potential the electropolymerization was executed for 1 s, 10 s, 1 min, and 15 min, respectively. The current changes after the addition of DHA for different electropolymerization potentials and times are shown in Figure 5.11. The resulting data is fairly scattered with no clear trend, and the current changes are below 2.5 μA for all cases. We conclude that the current response between DHA and the immobilized viologen polymer was not significant, though it was not zero and was an oxidation rather than reduction current.

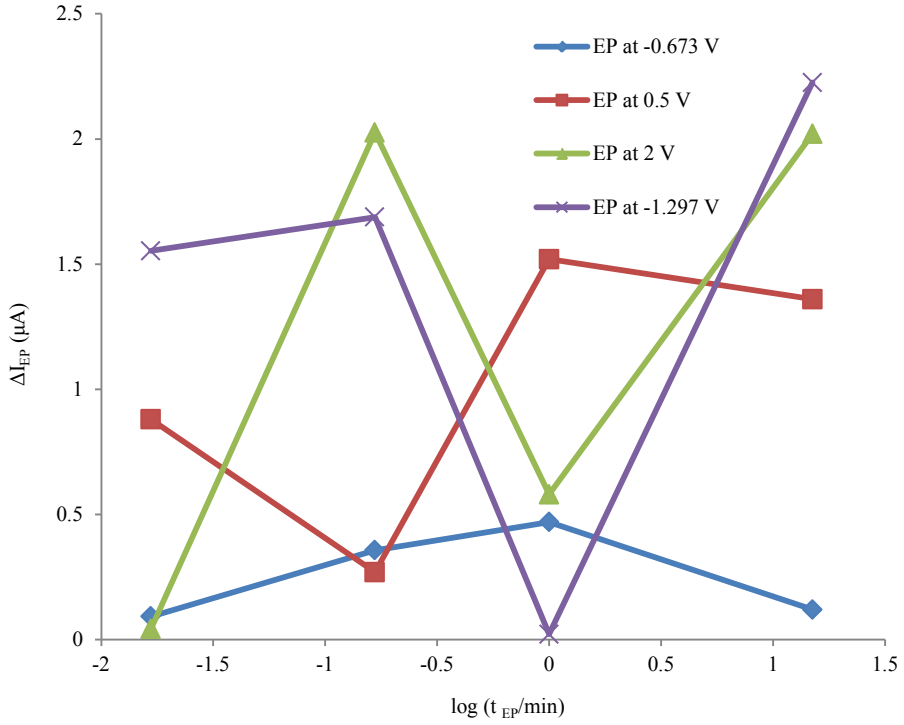

Figure 5.11 Electroactivity investigation of the immobilized viologen polymer for different electropolymerization (EP) treatments. The vertical axis is the current change after adding DHA to the cell; the horizontal axis is electropolymerization time. Lines are a guide to the eye.

5.3.3 Hypothesis Tests for the Low Catalytic Activity

There are several possibilities that could explain the low activity of the immobilized viologen polymer toward the carbohydrate oxidation. Our initial hypotheses were that the viologen monomer or its polymer may be not electroactive to oxidize carbohydrates, and the viologen-polymer coating may act as an insulation layer that blocks electron transfer. We designed the following experiments to test these hypotheses.

Fuel cell test of soluble viologen monomer: It was shown in Chapter 4 that the viologen monomer is redox active with a metal electrode. Here, we wished to determine if the soluble AAPB monomer is electroactive toward the oxidation of carbohydrates. Figure 5.12 shows the

electrocatalytic response of the viologen monomer after being added to the fuel cell with the presence of fructose.

The solution in the experiment shown in Figure 5.12 contained KOH and fructose, which were sequentially added to the cell. 7μL of 1 M KOH was first added. The working electrode was then set 0 V vs. Ag/AgCl, and recording for the test began. After the system was stabilized, 300 μL of 3 M fructose (0.9 mmole) was added to the cell with each addition of 100 μL for a total of 3 times using a 100 μL syringe. When the current was not changing, 0.02 g (0.05 mmole) of viologen monomer was then added to the cell.

As shown in Figure 5.12, the initial increase in current was caused by the addition of fructose that was likely to be oxidized by the residual oxygen in the cell or by the working electrode itself. After the viologen monomer addition, there was additional current generated, meaning that the viologen monomer is electroactive toward carbohydrate oxidation. Also observed was a change in solution color to intense purple showing that viologen is being reduced. The cell was run for 18 hours. The max current was reached within 2 hours; the current declined slowly and steadily as the fuel was exhausted. The coulombic efficiency over the course of 18 hours was 6.35% for the oxidation of fructose by the viologen monomers.

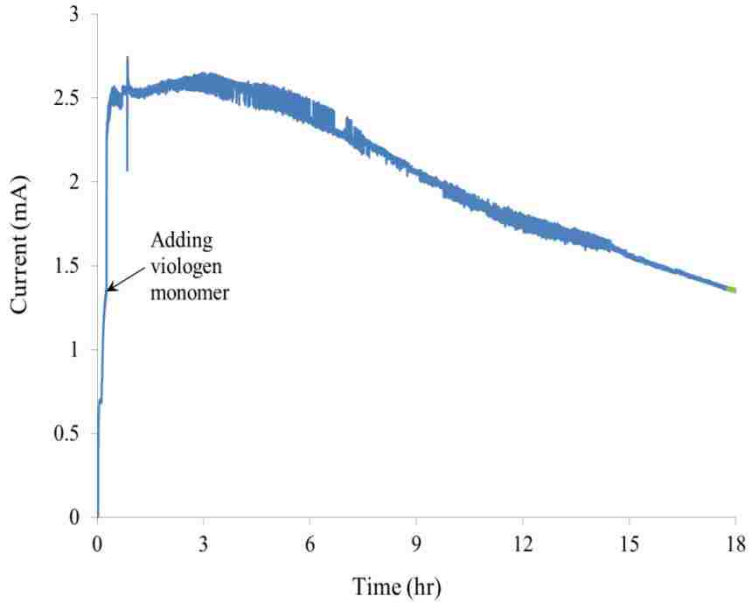

(a)

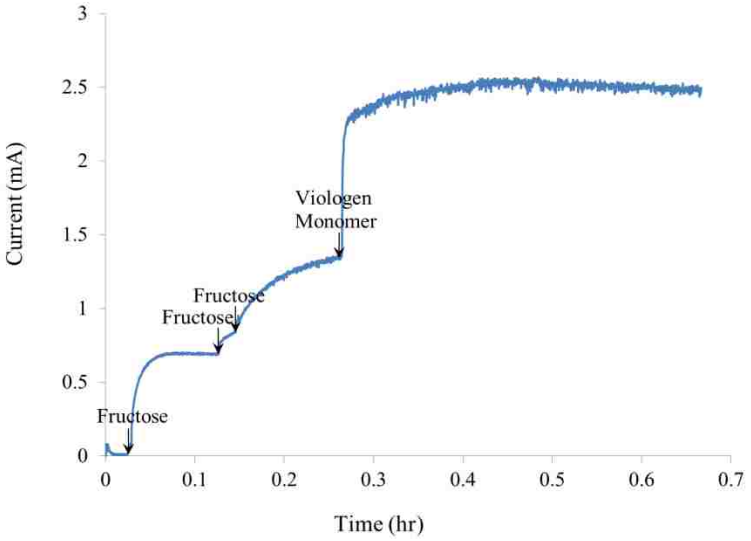

(b)

Figure 5.12 Plot of the current generated by soluble AAPB monomer oxidizing fructose. (a) Complete experiment, (b) magnification of short time results.

<u>Fuel cell test of viologen polymer in solution:</u> An experiment was designed to test if the viologen polymer was electroactive to oxidizing carbohydrates in an alkaline solution. It was

shown that the immobilized viologen polymer has a low catalytic activity; here, we wished to test if the solubilized viologen polymer is electroactive toward carbohydrate oxidation. Viologen polymers and oligomers are a by-product of the process to make the monomer. The polymer used in this experiment was taken straight from the production of viologen monomer synthesized without any polymerization inhibitor. The raw polymer product was washed with acetone and chloroform to remove any unreacted 4'4-bipyridium, and then was rotovapped to remove the residual solvent in order to obtain the net weight. The degree of polymerization was not known. The experiment was conducted with the same fuel cell setup for immobilized viologen polymer shown in Figure 5.1. A polished uncoated graphite disk was inserted in the rotation disk electrode holder as the working electrode.

Details of the experiment are as follows. 5 mL of quasi-anaerobic 1 M KOH was added to the cell, while maintaining a low oxygen environment in the fuel cell closure bag. The reference electrode was then placed in the cell and the rotating disk electrode was inserted into the anode compartment. The working electrode was set at 0 V and recording for the experiment began. 0.226 g of viologen polymer was first dissolved in 0.5 mL of double-distilled water, and then added to the cell once the current was stabilized. Lastly, 100 μL of 0.5 M DHA was added to the cell.

Figure 5.13 shows the current generated after DHA was added to the cell and reacted with the viologen polymer. The current response confirmed that the viologen polymer in solution is electroactive to oxidizing carbohydrate fuel in an alkaline solution. Furthermore, if we assume the viologen polymer was entirely made of viologen monomer units, the mole ratio of viologen monomer units to DHA is 13:1, which is 25 times more than the ratio of methyl viologen to DHA included in the later discussion. However, the current generated by the viologen polymer is

3 times less than that by methyl viologen oxidizing the same amount of DHA. The coulombic efficiency over the course of 6 hours was 1.1%, which is lower compared to that of soluble monomer. Partly because there was a higher ratio of catalyst to carbohydrate for the soluble viologen monomer experiment, namely 0.056 than that for the soluble polymer experiment, namely 0.0133. The low current production and coulombic efficiency were in an agreement with the fact that the viologen polymer has a lower mobility compared to those of methyl viologen and AAPB monomer. As reported in Chapter 4 the viologen monomer has a low heterogeneous electron-transfer rate k_{et}, this can be also applied to its polymer or even at a lower value.

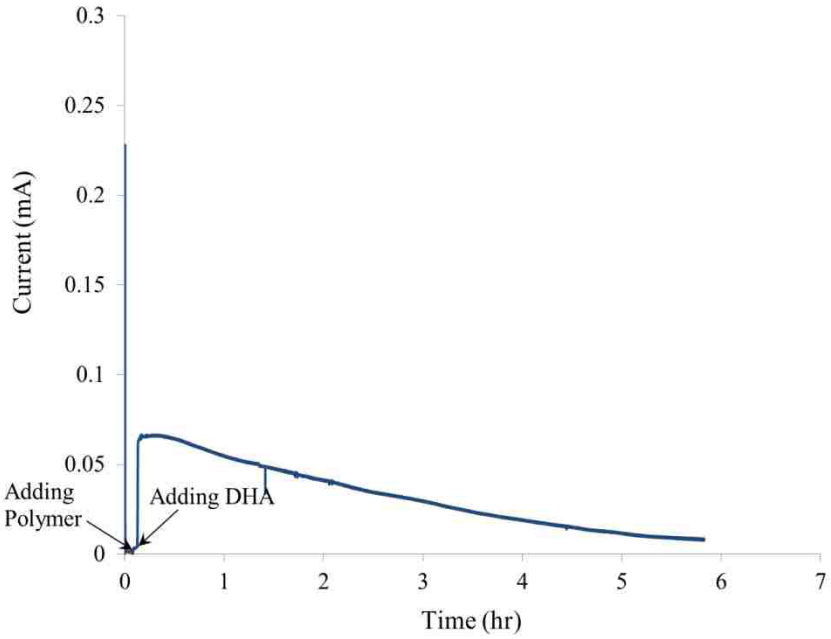

Figure 5.13 Plot of current generated by viologen polymer oxidizing DHA.

Polymer coating insulation test: Since both viologen monomer and polymer are electroactive to oxidizing carbohydrates in alkaline conditions, the last hypothesis to test is whether the viologen-polymer coating formed on the graphite disk blocks electron transfer and therefore acts an insulation layer. This test consisted of two experiments, one with the graphite

disk having been electropolymerized for 15 minutes, and the other one with a blank graphite disk for the purpose of control.

Both experiments were conducted using the fuel cell setup as shown in Figure 5.1. 6 mL of quasi-anaerobic 1 M KOH was added to the anode compartment, followed by placing the reference electrode and inserting the rotating disk electrode in the cell. The cell was then set at 0 V. Once the current stopped changing, 10 μL of saturated methyl viologen was added to the cell. When the current reached to stabilization again, 100 μL of DHA was last added.

Figure 5.12 shows the current responses after adding DHA to the cell with the presence of methyl viologen for the (a) blank graphite disk and (b) viologen-polymer-coated graphite disk. A sharp increase of current was observed for the control experiment upon the addition of DHA, and this was also seen for the polymer-coated graphite disk. The increases of the current are almost identical. Moreover, the coulombic efficiency over the course of 6 hours was 2.1% for the blank graphite disk and 2.2% for the polymer-coated graphite disk. The results confirm that the polymer coating is not acting as an insulation layer.

We have showed that the viologen monomer and viologen polymer are electroactive toward oxidizing carbohydrates, and the viologen polymer is not an insulation layer on the graphite disk. This leads us to conclude that the viologen moieties may undergo some chemical changes that dramatically weaken their catalytic ability to carbohydrates after immobilized on the surface, or that the way of the viologen groups oriented in the polymer during immobilization makes the viologen moieties isolated for carbohydrate molecules to reach. Because of the time limitation for this work, these hypotheses were not investigated here and are recommended for future work.

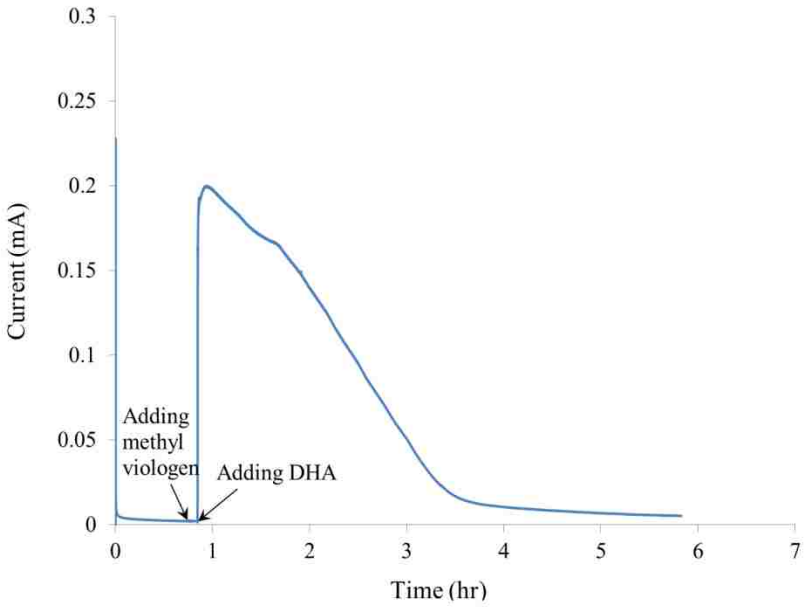

(a)

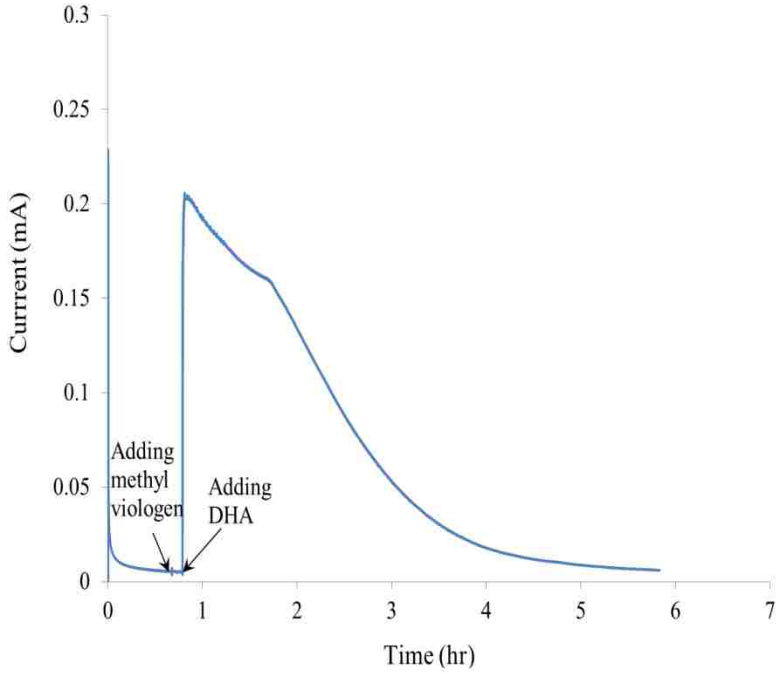

(b)

Figure 5.12 Plot of current generated by methyl viologen oxidizing DHA using the (a) blank graphite disk and (b) viologen-polymer-coated graphite disk as the working electrodes.

5.4 Conclusion

The AAPB viologen monomer was immobilized on gold and graphite surfaces by electro-reductive polymerization. The polymerization was carried out at a negative potential of -1.297 V vs. Ag/AgCl for 15 minutes in the presence of Zn^{2+}. SEM examination of the surface verified the polymer coating formation on the surfaces. The immobilization was also verified by detection of N element on the surfaces by EDAX, water contact angle measurement and XPS. The fuel cell test of the immobilized viologen polymer on graphite disks showed a low catalytic ability toward the oxidation of carbohydrate fuel.

To discover the cause of the low catalytic ability, additional tests were done. The results showed that the soluble viologen monomer and the viologen polymer in solution are electroactive to oxidizing carbohydrates, and the immobilized viologen polymer is not an insulation layer on the graphite surface.

6 Summary and Recommendations for Future Work

6.1 Summary

The primary goals of this work were to develop an immobilization chemistry of viologen on an electrode surface, and to study the electroactivity of the immobilized viologen for use as an electro-catalyst in a direct carbohydrate fuel cell (DCFC). This work has achieved the goals starting from synthesizing a novel viologen monomer to the determination of electrochemical properties of this monomer and to the development of the immobilization technique of this monomer on an electrode surface.

Chapter 3 reported on the synthesis and analysis of two new viologen molecules and a novel viologen monomer. The two new viologens are aminopropyl viologen (APV) and methylaminopropyl viologen (MAV), which were developed for the investigation of the electrochemical properties for mono- and di-substituted viologens in joint work with another student [20]. The novel viologen monomer (AAPB) was made for the intention of polymerization and immobilization, as reported in Chapter 5. NMR spectroscopy analysis was also included to verify the formation of each molecule.

Chapter 4 provided information on the cyclic voltammetry (CV) study of APV, MAV and the viologen monomer. Subsequently, electrochemical properties, including diffusion coefficients (D) and heterogeneous electron-transfer rate constants (k_{et}), were determined for each of these viologen molecules according to their corresponding CVs. The reported CVs for

APV and MAV were based on the work done in Ref. 20, and the values of D and k_{et} for these and other viologens were reported here. A CV test showed that the viologen monomer is electroactive in both aqueous and organic solvent. It was found that the monomer in its soluble form has similar or even greater diffusivity compared to other viologen molecules, but has much lower k_{et} values.

Chapter 5 described the immobilization chemistry of the AAPB viologen monomer on gold and graphite surfaces by electropolymerization, and the electroactivity of the immobilized polymer toward oxidizing carbohydrates. SEM images confirmed the formation of the viologen polymer coating on gold and graphite electrode surfaces. EDAX, water contact angle measurement, and XPS further verified the immobilization of the viologen polymer. However, the fuel cell tests showed a low catalytic activity to oxidize carbohydrates. Additional tests were performed to explore the cause; and the results showed that the soluble viologen monomer and viologen polymer in solution are catalytic active to oxidizing carbohydrates, and that the immobilized viologen-polymer coating is not an insulation layer. It is unclear at this point why the immobilized viologen polymer has a low catalytic activity toward oxidizing carbohydrates. There are a couple of further hypotheses to explore, which are included as a part of future work discussed below.

6.2 Future Work

The following work is recommended to continue investigating the low catalytic activity of the immobilized viologen polymer. This may include examining any chemical change of the viologen moieties during immobilization, and the arrangement of viologen moieties in the polymer. Chemical change could make the viologen inactive or weaken its catalytic activity to

oxidize carbohydrates. The physical arrangement of viologen moieties in the polymer is also an important factor to consider; steric hindrance could make it hard for viologen moieties and carbohydrate molecules to approach each other. NMR spectroscopy is a useful instrument to observe the chemical change of the viologen moieties on the molecular level. However, it would be hard to study the immobilized polymer on a surface; therefore it is recommended that the formed viologen polymer on an electrode surface should be scratched off and then dissolved in solvent for NMR examination. The challenge is to get enough amount of polymer off the surface for this assessment.

In addition, the unremoved Zn may be another factor that causes the low activity of the immobilized viologen polymer, as the residual Zn metal might possibly interfere with the oxidation of carbohydrate by the viologen moieties. To test this hypothesis, it is recommended to carry out a fuel cell experiment using the same device as shown in Figure 5.1, and using a Zn metal disk as the working electrode embedded in the rotating disk electrode holder. The test should be performed at 0 V vs. Ag/AgCl under nitrogen atmosphere and with DHA or other carbohydrates as fuel. Alternatively, one can place Zn ions in solution to see if the solubilized Zn could interact with the carbohydrate oxidation by the immobilized viologen polymer.

Once the immobilized viologen polymer shows a reasonable catalytic activity to the carbohydrate oxidation, co-electropolymerization of the viologen monomer with other molecules that have terminal acrylamide groups is recommended. The co-electropolymerization is to optimize the surface density of viologen groups on the surface. High viologen density may not be desirable because of the steric hindrance that can encumber the electron transfer. On the other hand, low viologen density can lower the fuel cell efficiency.

Bibliography

[1] D. R. Wheeler, J. Nichols, D. Hansen, M. Andrus, S. Choi, and G. D. Watt, Journal of the Electrochemical Society, vol. 156, pp. B1201-B1207, 2009.

[2] J. H. Kim, W. Park, and S. Kim, Bulletin of the Korean Chemical Society, vol. 32, pp. 3849-3850, Nov 2011.

[3] G. D. Watt, D. Hansen, D. Dodson, M. Andrus, and D. Wheeler, Renewable Energy, vol. 36, pp. 1523-1528, May 2011.

[4] F. W. Schenck, "Glucose and Glucose-Containing „," in Syrups in Ullmann's Encyclopedia of Industrial Chemistry 2006, ed: Wiley-VCH, 2006.

[5] P. C. Badger, "Ethanol from cellulose: A general review," in Trends in new crops and new uses, ed Alexandria, VA. : ASHS Press, 2002, pp. 17–21.

[6] Ethanol industry statistics. Available: http://www.ethanolrfa.org/pages/statistics/#E

[7] Petroleum Product Prices. Available: http://www.eia.gov/oiaf/aeo/tablebrowser/#release=AEO2013ER&subject=0-AEO2013ER&table=12-AEO2013ER&region=0-0&cases=full2012-d020112c,early2013-d102312a

[8] Table 3b--World raw sugar price, ICE Contract 11 nearby futures price, monthly, quarterly, and by calendar and fiscal year 1/ [Online]. Available: http://ers.usda.gov/topics/food-markets-prices.aspx

[9] W. P. Dean Wheeler, unpublished, 2010.

[10] R. A. Bullen, T. C. Arnot, J. B. Lakeman, and F. C. Walsh, Biosensors & Bioelectronics, vol. 21, pp. 2015-2045, May 2006.

[11] F. Davis and S. P. J. Higson, Biosensors & Bioelectronics, vol. 22, pp. 1224-1235, Feb 2007.

[12] S. Kerzenmacher, J. Ducree, R. Zengerle, and F. von Stetten, Journal of Power Sources, vol. 182, pp. 1-17, Jul 2008.

[13] A. T. Yahiro, S. M. Lee, and D. O. Kimble, Biochimica Et Biophysica Acta, vol. 88, pp. 375-&, 1964.

[14] S. Ernst, J. Heitbaum, and C. H. Hamann, Berichte Der Bunsen-Gesellschaft-Physical Chemistry Chemical Physics, vol. 84, pp. 50-55, 1980.

[15] I. Becerik and F. Kadirgan, Journal of Electroanalytical Chemistry, vol. 436, pp. 189-193, Oct 1997.

[16] J. McGinley, F. N. McHale, P. Hughes, C. N. Reid, and A. P. McHale, Biotechnology Letters, vol. 26, pp. 1771-1776, Dec 2004.

[17] K. Rabaey, G. Lissens, S. D. Siciliano, and W. Verstraete, Biotechnology Letters, vol. 25, pp. 1531-1535, Sep 2003.

[18] K. Rabaey and W. Verstraete, Trends in Biotechnology, vol. 23, pp. 291-298, Jun 2005.

[19] W. Z. S. You, J. Jiang, and S. Zhoa,, J. Power Sources, vol. 162, p. 1409 2006.

[20] A. Read, D. Hansen, S. Aloi, W. G. Pitt, D. R. Wheeler, and G. D. Watt, Renewable Energy, vol. 46, pp. 218-223, Oct 2012.

[21] D. C. Hansen, Y. N. Pan, J. Stockton, W. G. Pitt, and D. R. Wheeler, Journal of the Electrochemical Society, vol. 159, pp. H834-H841, 2012.

[22] Types of Fuel Cells. Available: http://www.fuelcells.org/fuel-cells-and-hydrogen/types/

[23] Fuel Cell. Available: http://en.wikipedia.org/wiki/Fuel_cell

[24] E. B. P. Schechner, and L. Mor, presented at the FUEL CELL 2005, Third International Conference on Fuel cell Science, Engineering and Technology, 2005.

[25] Z. W. Chen, D. Higgins, A. P. Yu, L. Zhang, and J. J. Zhang, Energy & Environmental Science, vol. 4, pp. 3167-3192, Sep 2011.

[26] K. Wiesener, D. Ohms, V. Neumann, and R. Franke, Materials Chemistry and Physics, vol. 22, pp. 457-475, Jul 1989.

[27] S. Baranton, C. Coutanceau, E. Garnier, and J. M. Leger, Journal of Electroanalytical Chemistry, vol. 590, pp. 100-110, May 2006.

[28] J. A. R. Vanveen and C. Visser, Electrochimica Acta, vol. 24, pp. 921-928, 1979.

[29] A. Ishihara, Y. Ohgi, K. Matsuzawa, S. Mitsushima, and K. Ota, Electrochimica Acta, vol. 55, pp. 8005-8012, Nov 2010.

[30] R. Jasinski, Nature, vol. 201, pp. 1212-&, 1964.

[31] L. Michael, Chemical Review, vol. 16, pp. 243-290, 1935.

[32] P. M. S. Monk, The Viologen Physicochemeical Properties, Synthesis and Application of the Salts of 4,4' Bipyridine. Chichester: John Wiley&Sons, 1998.

[33] C. L. Bird, Kuhn, A.T., Chemical Society Review, vol. 10, pp. 49-82, 1981.

[34] J. Volke, Collection of Czechoslovak Chemical Communications, vol. 33, pp. 3044-&, 1968.

[35] L. Pospisil, J. Kuta, and J. Volke, Journal of Electroanalytical Chemistry, vol. 58, pp. 217-227, 1975.

[36] A. Factor and G. E. Heinsohn, Journal of Polymer Science Part B-Polymer Letters, vol. 9, pp. 289-&, 1971.

[37] H. Sato and T. Tamamura, Journal of Applied Polymer Science, vol. 24, pp. 2075-2085, 1979.

[38] H. T. Vandam and J. J. Ponjee, Journal of the Electrochemical Society, vol. 121, pp. 1555-1558, 1974.

[39] M. S. Simon and P. T. Moore, Journal of Polymer Science Part a-Polymer Chemistry, vol. 13, pp. 1-16, 1975.

[40] T. Endo, A. Kameyama, Y. Mambu, Y. Kashi, and M. Okawara, Journal of Polymer Science Part a-Polymer Chemistry, vol. 28, pp. 2509-2516, Aug 1990.

[41] H. C. Chang, M. Osawa, T. Matsue, and I. Uchida, Journal of the Chemical Society-Chemical Communications, pp. 611-612, May 1991.

[42] V. Jain, M. Khiterer, R. Montazami, H. M. Yochum, K. J. Shea, and J. R. Heflin, Acs Applied Materials & Interfaces, vol. 1, pp. 83-89, Jan 2009.

[43] M. Inaba, Z. Ogumi, and Z. I. Takehara, Journal of the Electrochemical Society, vol. 141, pp. 2579-2586, Oct 1994.

[44] I. Yamaguchi and T. Asano, Journal of Materials Science, vol. 46, pp. 4582-4587, Jul 2011.

[45] I. Yamaguchi, S. Shigesue, and M. Sato, Reactive & Functional Polymers, vol. 69, pp. 91-96, Feb 2009.

[46] L. P. Zhao, K. G. Neoh, and E. T. Kang, Chemistry of Materials, vol. 14, pp. 1098-1106, Mar 2002.

[47] J. Song, Z. Hong, R. Nagarale, and W. Shin, Journal of Electrochemical Science and Technology, vol. 2, pp. 163-167, 2011.

[48] E. Katz, A. L. Delacey, J. L. G. Fierro, J. M. Palacios, and V. M. Fernandez, Journal of Electroanalytical Chemistry, vol. 358, pp. 247-259, Nov 1993.

[49] H. Munstedt, Polymer, vol. 27, pp. 899-904, Jun 1986.

[50] P. M. S. Monk, Fundamentals of Electroanalytical Chemistry. Chichester: John Wiley & Sons Ltd, 2001.

[51] D. T. Sawyer, A. Sobkowiak, J. Julian, and L. Roberts, Electrochemistry for Chemists. New York: John Wiley & Sons, 1995.

[52] V. S. Bagotsky, Fundamentals of Electrochemistry. Hoboken, New Jersey: John Wiley & Sons, Inc., 2006.

[53] J. David K. Gosser, Cyclic Voltammetry Simulation and Analysis of Reaction Mechanisms. New York: VCH Publishers, Inc., 1994.

[54] J. Newman and K. E. Thomas-Alyea, Electrochemical Systems, 3rd ed. Hoboken, New Jersey: John Wiley & Sons, 2004.

[55] R. T. Bibart, K. W. Vogel, and D. G. Drueckhammer, Journal of Organic Chemistry, vol. 64, pp. 2903-2909, Apr 1999.

[56] J. R. Mohrig, C. N. Hammond, and P. F. Schatz, Techniques in Organic Chemistry New York: W. H. Freeman and Company, 2010.

[57] R. M. Silverstein and F. X. Webster, Spectrometic Identification of Organic Compounds Sixth ed. New York: John Wiley & Sons, Inc., 1998.

[58] N. G. Tsierkezos, Journal of Solution Chemistry, vol. 36, pp. 1301-1310, Oct 2007.

[59] J. E. B. Randles, Transactions of the Faraday Society, vol. 44, pp. 322-327, 1948.

[60] R. B. Bird, W. E. Stewart, and E. N. Lightfoot, Transport Phenomena, Revised 2nd Edition ed. New York: John Wiley & Sons, Inc, 2007.

[61] Nicholso.Rs, Analytical Chemistry, vol. 37, pp. 1351-&, 1965.

[62] N. K. Bhatti, M. S. Subhani, A. Y. Khan, R. Qureshi, and A. Rahman, Turkish Journal of Chemistry, vol. 29, pp. 659-668, 2005.

[63] G. L. Collins and N. W. Thomas, Journal of Polymer Science Part a-Polymer Chemistry, vol. 15, pp. 1819-1831, 1977.

[64] S. N. Bhadani and S. Kundu, journal of polymer materials, vol. 1, pp. 31-43, 1984.

[65] J. F. S. M. C. Zerner, United States Patent, 1969.

[66] Y. H. Tang, K. X. Pan, X. J. Wang, C. B. Liu, and S. L. Luo, Microchimica Acta, vol. 168, pp. 231-237, Mar 2010.

[67] J. Goldstein, D. Newbury, D. Joy, C. Lyman, P. Echlin, E. Lifshin, L. Sawyer, and J. Michael, Scanning Electron Microscopy and X-ray Microanalysis, 3rd ed. New York: Springer Science and Business Media, Inc, 2003.

[68] D. Hansen, D. Wheeler, and W. G. Pitt, unpublished, 2013.

Appendix

This appendix describes the method used to determine values of ψ for AAPB viologen monomer included in Chapter 4. ψ is the kinetic parameter reported in Nicholson paper [61], and it can be obtained from the peak-potential separation ΔE_p. A table in Nicholson paper reported the variation of ψ with ΔE_p, Figure A.1 is a plot of the data reported in that table in a log scale with a fitted line.

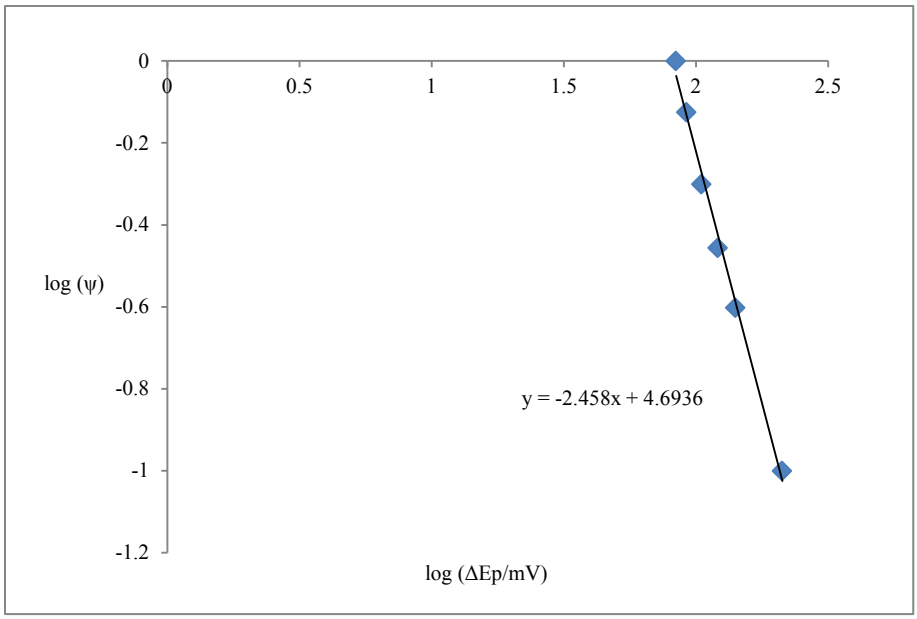

Figure A.1 Plot of data as reported in Nicholson paper [61] on variation of kinetic parameter (ψ) with peak potential separation (ΔE_p) in a log scale.

For AAPB monomer, the values of ΔE_p were determined from the cyclic voltammograms shown in Figure 4.4, the corresponding ψ values at each scan rate in aqueous and DMSO solutions were then extrapolated from the fitted line as shown above.